CHAPTER 1

Basic Optical Calculations

> An excellent plumber is infinitely more admirable than an incompetent philosopher. The society which scorns excellence in plumbing because plumbing is a humble duty and tolerates shoddiness in philosophy because it is an exalted activity will have neither good plumbing nor good philosophy. Neither its pipes nor its theories will hold water.
>
> —John W. Gardner[†]

1.1 INTRODUCTION

Okay, we've decided to build an electro-optical system. It's going to be so great that everybody who sees it will hate us. Now comes the fun part, the planning and designing, and then the hard part, the building and testing. To design and plan, we have to have some way of knowing how our brainchild ought to behave before it is built—that is, theory.

At the conceptual stage, the measurement principle is poorly understood and many quite different schemes are suggesting themselves. To make sense of it, you need a white board and a couple of smart and experienced colleagues to bounce ideas off, plus some pointers on how to begin. The aim of this chapter is to equip you to do a conceptual instrument design on the back of an envelope. It assumes some background in optics, especially some acquaintance with plane waves and Fourier transforms.

The indispensable ingredients of a conceptual design are:

- A measurement idea
- Operational requirements (field of view, scan speed, spot size, sensitivity, etc.)
- A photon budget
- A rough optical design
- A detection strategy
- A signal processing strategy

[†]John W. Gardner, *Excellence, Can We Be Equal and Excellent Too?* Harper, New York, 1961, p. 86.

Building Electro-Optical Systems, Making It All Work, Second Edition, By Philip C. D. Hobbs
Copyright © 2009 John Wiley & Sons, Inc.

The best way to get them is through several sessions at that white board, with a lot of thought and calculation in between. (It is amazing how many people think they've finished with engineering calculations when they hand in their last exam, but that attitude is sudden death in the instrument-building business.) Once you have these, you can make a list of the main technical risks, in descending order of hairiness, and pretty soon you have a plan for how to proceed. The size of these technical risks is important—they can range from finding parts to violating laws of physics. Right at the beginning, we must decide whether the measurement is even possible, which requires more imagination than analysis. The invention of two-photon Doppler-free spectroscopy is a good example.

Example 1.1: Two-Photon Doppler-Free Spectroscopy.[†] Gas-phase spectroscopy is limited at low pressure by the random thermal motions of the gas molecules, and at high pressures by their collisions. Molecules with different speeds along the laser beam axis experience different Doppler shifts, so that their absorption features occur at different frequencies in the lab frame, leading to *Doppler broadening*. A two-photon transition involves the absorption of two photons, whose energies must sum to the transition energy. The absorption (and any resulting fluorescence) can be modulated by chopping the excitation beam. By using two excitation beams going in opposite directions, some events will involve absorption of one photon from each beam, which can occur only when both beams are unblocked by their choppers. If the modulation frequencies of the two beams are different, this part of the signal will appear at the sum and difference of the chopping frequencies. If a molecule has nonzero speed along the beam, then to leading order in V/c, it will see each beam shifted by

$$\Delta\nu_i = \frac{-\mathbf{k}_i \cdot \mathbf{v}}{2\pi}. \tag{1.1}$$

Since the two beams have oppositely directed $\mathbf{k}$ vectors, one will be upshifted and the other downshifted by the same amount; the sum of the photon energies, $h(\nu_1 + \nu_2)$, is unshifted. Thus these mixing components are present only when the laser is tuned exactly to the rest-frame resonance frequency—they show no first-order Doppler broadening. An apparently inherent physical limit is circumvented with an extra chopper and a mirror or two; such is the power of a good measurement idea.

Once the idea is in hand, analysis is needed, to decide between competing alternatives. Such feasibility calculations are at the heart of electro-optical systems lore, and their most important fruit is a highly trained intuition, so we'll do lots of examples. The places where assumptions break down are usually the most instructive, so we'll also spend some time discussing some of the seedier areas of optical theory, in the hope of finding out where the unexamined assumptions lurk. We'll begin with wave propagation and imaging.

[†]This example is adapted from L. S. Vasilenko, V. P. Chebotaev, and A. V. Shishaev, *JETP Lett*. **3** (English translation), 161 (1970).

1.2 WAVE PROPAGATION

1.2.1 Maxwell's Equations and Plane Waves

Any self-respecting book on optics is obliged to include Maxwell's equations, which are the complete relativistic description of the electromagnetic field *in vacuo* and are the basis on which all optical instruments function. They are also useful for printing on T-shirts. Fortunately, this is a book of practical lore, and since Maxwell's equations are almost never used in real design work, we don't need to exhibit them. The most basic equation that is actually useful is the *vector wave equation*,

$$\nabla^2\mathbf{E} - \frac{1}{c^2}\frac{\partial^2\mathbf{E}}{\partial t^2} = 0, \tag{1.2}$$

where c is the speed of light. Most of the time we will be calculating a monochromatic field, or at least a superposition of monochromatic fields. We can then separate out the time dependence as $\exp(-i\omega t)$ and write $k = \omega/c$, leaving the vector Helmholtz equation,

$$(\nabla^2 + k^2)\mathbf{E} = 0. \tag{1.3}$$

Its simplest solution is a vector plane wave,

$$\mathbf{E}(\mathbf{x}) = \mathbf{E}_0 e^{i\mathbf{k}\cdot\mathbf{x}} \tag{1.4}$$

where the two fixed vectors are $\mathbf{E}_0$, the electric field vector, which may be complex, and $\mathbf{k}$ is the *wave vector*, whose magnitude $k = |\mathbf{k}| = \omega/c$ is called the *propagation constant*. If $\mathbf{E}_0$ is real, the field is said to be *linearly polarized* along $\mathbf{E}_0$; if its real and imaginary parts are the same size, so that the instantaneous $\mathbf{E}$ rotates without changing length, the field is *circularly polarized*; otherwise, it's *elliptically polarized* (see Section 1.2.8).

Power flows parallel to $\mathbf{k}$ in an isotropic medium, but need not in an anisotropic one, so it is separately defined as the *Poynting vector* $\mathbf{S} = \mathbf{E} \times \mathbf{H}$ (see Sections 4.6.1 and 6.3.2). In the complex notation, the one-cycle average Poynting vector is $\mathbf{S} = \mathrm{Re}[\mathbf{E} \times \mathbf{H}^*]$.

1.2.2 Plane Waves in Material Media

So far, we have only considered propagation *in vacuo*. Electromagnetics in material media is enormously complicated on a microscopic scale, since there are $\sim 10^{22}$ scatterers/cm^3. Fortunately, for most purposes their effects are well approximated by mean field theory, which smears out all those scatterers into a jelly that looks a lot like vacuum except for in a change in the propagation velocity, the E/H ratio, and some loss. A plane wave entering a material medium via a plane surface remains a plane wave, with different $\mathbf{k}$ and $\mathbf{E}_0$.

In a medium, light travels at a speed $v = c/n$. The constant n, the *refractive index*, is given by $n = \sqrt{\mu_r \epsilon_r}$, where μ_r and ϵ_r are the relative magnetic permeability and dielectric constant of the material at the optical frequency, respectively. Since μ_r is nearly always 1 in optics, $n = \sqrt{\epsilon_r}$. In addition, the material will change the *wave impedance*, $Z = E/H = \sqrt{\mu/\epsilon} = (120\pi\ \ \Omega)\sqrt{\mu_r/\epsilon_r}$. The analogy between wave impedance and transmission line impedance is a fruitful one.

In absorbing media, the refractive index is complex.[†] Assuming the medium is linear and time invariant, the temporal frequency cannot change, so k is different in the medium; the new k is $k_n = nk_0$, where k_0 is the vacuum value. We usually drop the subscripts, so k is taken to be in the medium under consideration.

There are one or two fine points deserving attention here. One is that n is not constant with ω, a phenomenon known as *dispersion*. Besides making light of different colors behave differently, this leads to distortion of a time-modulated signal. The carrier wave propagates at the *phase velocity* $v_p = \omega/k$, but the envelope instead propagates, approximately unchanged in shape, at the *group velocity* v_g, given by

$$v_g = \partial\omega/\partial k. \tag{1.5}$$

Since the carrier propagates at the phase velocity v, as an optical pulse goes along its carrier "slips cycles" with respect to its envelope; that's worth remembering if you build interferometers. The group velocity approximation (1.5) holds for short propagation distances only, that is, when the difference Δt in the transit times of different frequency components is much less than the pulse width τ. In the opposite limit, where $\Delta t \gg \tau$, the output is a time Fourier transform of the input pulse.[‡]

The other fine point is that ϵ_r is in general a tensor quantity; there is no guarantee that the response of the material to an applied electric field is the same in all directions. In this book we're concerned only with the linear properties of optical systems, so a tensor is the most general local relationship possible. The resulting dependence of n on polarization leads to all sorts of interesting things, such as *birefringence* and *beam walkoff*. There are in addition strange effects such as *optical activity* (also known as *circular birefringence*), where the plane of polarization of a beam rotates slowly as it propagates. We'll talk more about these weird wonders in Chapters 4 and 6.

Aside: The Other Kind of Polarization. The dielectric constant ϵ_r expresses the readiness with which the charges in the medium respond to the applied electric field; it is given by $\epsilon_r = 1 + 4\pi\chi$, where χ is the electric susceptibility (zero for vacuum); the electric polarization $\mathbf{P}$ is $\epsilon_0\chi\mathbf{E}$. This is a different usage than the usual optical meaning of polarization, and it's worth keeping the two distinct in your mind.

1.2.3 Phase Matching

The two basic properties of any wave field are amplitude and phase. At any point in space-time, a monochromatic wave has a unique phase, which is just a number specifying how many cycles have gone by since time $t = 0$. Since it's based on counting, phase is invariant to everything—it's a Lorentz scalar, so it doesn't depend on your frame of reference or anything else, which turns out to be a very powerful property. The requirement for phase matching at optical interfaces is the physical basis of geometrical optics. A plane wave has the unique property of being translationally invariant, meaning that if you move from one point to another, the only thing that changes is an additive

[†]Complex refractive index $\tilde{n}$ is often quoted as $n + ik$, where n and k are real and positive, but it is conceptually simpler to leave n complex, because the Fresnel formulas and Snell's law still work with absorbing media.

[‡]The impulse response of a linearly dispersive medium is a chirp, and the Fourier transform can be computed as the convolution of a function with a chirp. This turns out to be important in digital signal processing, where it leads to the chirp-Z transform.

phase shift (equivalent to a pure time delay). In particular, at a planar interface, moving the reference point within the plane cannot change the phase relationship between the fields on either side.

1.2.4 Refraction, Snell's Law, and the Fresnel Coefficients

If a plane wave encounters a plane interface between two semi-infinite slabs of index n_1 and n_2, as shown in Figure 1.1, the light is partially reflected and partially transmitted—a standard problem in undergraduate electromagnetics classes. We expect the fields to consist of an incident and a reflected plane wave on the input side and a single transmitted plane wave on the output side. Phase matching at the interface requires that the tangential **k** vectors of all the waves be the same, which reproduces the law of reflection for the reflected component and *Snell's law* for the transmitted one:

$$n_1 \sin\theta_1 = n_2 \sin\theta_2. \tag{1.6}$$

If there are m parallel planar interfaces, $\mathbf{k}_\parallel$ is the same in all the layers, so since (in the jth layer) $k_j = n_j k_0$, we can use the phase matching condition to get $k_\perp$ in the jth layer:

$$k_\perp^2 = n_j^2 k_0^2 - k_\parallel^2. \tag{1.7}$$

This is important in the theory of optical coatings. The continuity conditions on tangential **E** and perpendicular **D** across the boundary give the *Fresnel formulas* for the field amplitudes,

$$\frac{E_p''}{E_p} \equiv r_{p12} = -\frac{\tan(\theta_1 - \theta_2)}{\tan(\theta_1 + \theta_2)} = -\frac{n_2\cos\theta_1 - n_1\sqrt{1 - [(n_1/n_2)\sin\theta_1]^2}}{n_2\cos\theta_1 + n_1\sqrt{1 - [(n_1/n_2)\sin\theta_1]^2}}, \tag{1.8}$$

$$\frac{E_p'}{E_p} \equiv t_{p12} = \frac{2\sin\theta_1\cos\theta_2}{\sin(\theta_1 + \theta_2)} = \frac{2n_1\cos\theta_1}{n_2\cos\theta_1 + n_1\sqrt{1 - [(n_1/n_2)\sin\theta_1]^2}}, \tag{1.9}$$

for light linearly polarized (i.e., **E** lying) in the *plane of incidence*. This plane is defined by the surface normal $\hat{\mathbf{n}}$ (unrelated to n) and $\mathbf{k}_{\text{inc}}$. In Figure 1.1, it is the plane of

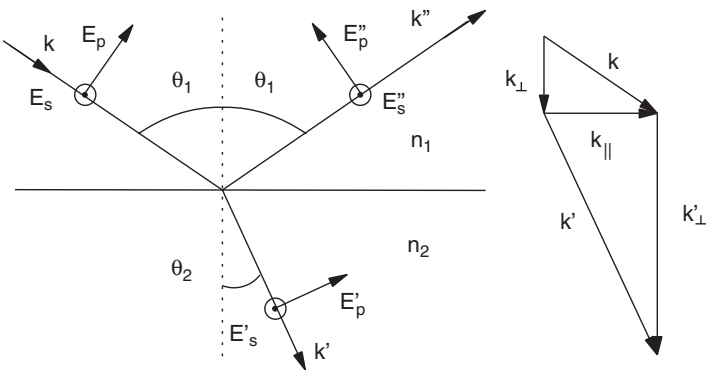

Figure 1.1. Refraction and reflection of a plane wave at a plane dielectric boundary. The angle of refraction θ_2 is given by Snell's law.

the page. For light linearly polarized perpendicular to the plane of incidence, these become

$$\frac{E_s''}{E_s} \equiv r_{s12} = -\frac{\sin(\theta_1 - \theta_2)}{\sin(\theta_1 + \theta_2)} = \frac{n_1 \cos\theta_1 - n_2\sqrt{1 - [(n_1/n_2)\sin\theta_1]^2}}{n_1 \cos\theta_1 + n_2\sqrt{1 - [(n_1/n_2)\sin\theta_1]^2}}, \tag{1.10}$$

$$\frac{E_s'}{E_s} \equiv t_{s12} = \frac{2\sin\theta_2 \cos\theta_1}{\sin(\theta_1 + \theta_2)} = \frac{2n_1 \cos\theta_1}{n_1 \cos\theta_1 + n_2\sqrt{1 - [(n_1/n_2)\sin\theta_1]^2}}. \tag{1.11}$$

The two polarizations are known as p and s, respectively. As a mnemonic, s polarization means that $\mathbf{E}$ *sticks* out of the plane of incidence.[†] The quantities r and t are the reflection and transmission coefficients, respectively. These *Fresnel coefficients* act on the amplitudes of the fields.[‡] The transmitted and reflected power ratios R and T, given by

$$R = |r|^2 \quad \text{and} \quad T = \frac{n_2 \cos\theta_2}{n_1 \cos\theta_1}|t|^2, \tag{1.12}$$

are known as the *reflectance* and *transmittance*, respectively.

The Fresnel coefficients have fairly simple symmetry properties; if the wave going from n_1 to n_2 sees coefficients r_{12} and t_{12}, a wave coming in the opposite direction sees r_{21} and t_{21}, where

$$\begin{aligned} r_{p21} &= -r_{p12}, \quad t_{p21} = (n_1 \cos\theta_1)/(n_2 \cos\theta_2)t_{p12}; \\ r_{s21} &= -r_{s12}, \quad t_{s21} = (n_2 \cos\theta_2)/(n_1 \cos\theta_1)t_{s12}. \end{aligned} \tag{1.13}$$

The symmetry expressions for t_{21} are more complicated because they have to take account of energy conservation between the two media.

1.2.5 Brewster's Angle

Especially sharp-eyed readers may have spotted the fact that if $\theta_1 + \theta_2 = \pi/2$, the denominator of (1.8) goes to infinity, so $r_p = 0$. At that angle, $\sin\theta_2 = \cos\theta_1$, so from Snell's law, $\tan\theta_1 = n_2/n_1$. This special value of θ_i is called *Brewster's angle* θ_B. Note that the transmitted angle is $\pi/2 - \theta_B$, which is Brewster's angle for going from n_2 into n_1. Brewster angle incidence with very pure p-polarized light is the best existing technique for reducing reflections from flat surfaces, a perennial concern of instrument designers (see Section 4.7.3).

Laser tube windows are always at Brewster's angle to reduce the round-trip loss through the cavity. The loss in the s polarization due to four high angle quartz–air surfaces is nearly 40% in each direction. Regeneration in the cavity greatly magnifies this gain difference, which is why the laser output is highly polarized. Brewster angle

[†]The s is actually short for *senkrecht*, which is German for perpendicular. The two polarizations are also called *TE* and *TM*, for *transverse electric* and *transverse magnetic*, that is, which field is sticking out of the plane of incidence. This nomenclature is more common in waveguide theory.

[‡]There is another sign convention commonly used for the p-polarized case, where the incident and reflected $\mathbf{E}$ fields are taken in opposite directions, yielding a confusing sign change in (1.8). We adopt the one that makes $r_p = r_s$ at normal incidence.

incidence is also commonly used in spectroscopic sample cells, Littrow prisms, and other high accuracy applications using linearly polarized, collimated beams.

Ideally, a smooth optical surface oriented at θ_B to the incoming p-polarized beam would reflect nothing at all, but this is not the case with real surfaces. Roughness and optical anisotropy make it impossible to make every single region encounter the light beam at the same angle or with the same refractive index, so there are always residual reflections even at θ_B. Surface layers also prevent complete canceling of the reflected wave, because the two will in general have different Brewster's angles and because of the phase delay between the reflections from the top and bottom of the layer. Below the critical angle, dielectric reflections always have phase 0 or π, so there's no way to tip the surface to get rid of a phase-shifted reflection.

Aside: Fossil Nomenclature. When Malus discovered polarization (in 1808) by looking at reflections from a dielectric, he quite reasonably identified the *plane of polarization* with the plane of incidence. This conflicts with our modern tendency to fix on the **E** field in considering polarization. There are still some people who follow Malus's convention, so watch out when you read their papers.

1.2.6 Total Internal Reflection

If $n_1 > n_2$, there exists an angle θ_C, the *critical angle*, where Snell's law predicts that $\sin\theta_2 = 1$, so $\theta_2 = \pi/2$: grazing incidence. It is given by

$$\theta_C = \arcsin(n_2/n_1). \tag{1.14}$$

Beyond there, the surds in the Fresnel formulas (1.8)–(1.11) become imaginary, so t vanishes and r sits somewhere on the unit circle (the reflectivity is 1 and the elements of $\mathbf{E}'$ become complex).

This *total internal reflection* (TIR) is familiar to anyone who has held a glass of water, or looked up at the surface while underwater. It is widely used in reflecting prisms. There are two things to remember when using TIR: the reflection phase is massively polarization dependent and the fields extend beyond the surface, even though there is no propagating wave there. A TIR surface must thus be kept very clean, and at least a few wavelengths away from any other surface.

By putting another surface sufficiently close by, it is possible to couple light via the evanescent field, a phenomenon called *frustrated TIR* or, more poetically, *evanescent coupling*. This is the optical analogue of quantum mechanical tunneling.

The reflection phase represents a relative time delay of the propagating wave. The s-polarized wave is delayed more, because it has a larger amplitude in the evanescent region, which requires more of a phase slip between the incident and reflected waves (remember the continuity conditions). This sort of physical reasoning is helpful in keeping sign conventions straight, although it is not infallible. The phase shift δ between s and p polarizations is[†]

$$\delta = \delta_s - \delta_p = -\arctan\frac{2\cos\theta_i\sqrt{\sin^2\theta_i - (n_2/n_1)^2}}{\sin^2\theta_i}. \tag{1.15}$$

[†]M. Born and E. Wolf, *Principles of Optics*, 6th ed. (corrected). Pergamon, Oxford, 1983, pp. 47–51.

1.2.7 Goos–Hänchen Shift

The angle-dependent phase shift on TIR functions much as dispersion does in the time domain, delaying different components differently. Dispersion causes the envelope of a pulse to propagate at the group velocity, which is different from the phase velocity. In the same way, the phase shift on TIR causes the envelope of a reflected beam to be shifted slightly in space from the incident beam, the *Goos–Hänchen shift*. It is less well known than the group velocity effect, mainly because the effect doesn't build up as it goes the way dispersion effects do, so the shift is small under normal circumstances, though large enough to cause image aberrations on reflection from TIR surfaces. The place it does become important is in multimode fiber optics, where a ray undergoes many, many reflections and the shift accordingly adds up.

The variation in the Goos–Hänchen shift comes from the speeding up of the wave that sticks out the most into the low index material. It is responsible for the apparently paradoxical behavior of optical fiber modes near cutoff (see Section 8.3.1). We expect high angle modes to slow down due to the decrease of k_z with angle—they spend more of their time bouncing back and forth instead of traveling down the fiber axis. In fact, they do slow down with increasing angle at first, but then speed up again as they near cutoff, when the wave sticks farther and farther out into the low index material. To leading order, the effect is the same as if the wave bounced off an imaginary surface one decay length into the low index material. Note that this does not contradict the last section; the phase shift is a delay, but the Goos–Hänchen shift makes the mode propagation anomalously fast.

1.2.8 Circular and Elliptical Polarization

What happens when the p and s components get out of phase with each other? The exponential notation, remember, is just a calculating convenience; real physical quantities always give real numbers. The instantaneous E-field strength is

$$E^2 = [\mathrm{Re}\{E_x e^{i\omega t}\}]^2 + [\mathrm{Re}\{E_y e^{i\omega t+\phi}\}]^2. \tag{1.16}$$

A linearly polarized monochromatic wave has an E that varies sinusoidally, passing through zero twice each cycle. When $\mathbf{E}$ has complex coefficients, the p and s components oscillate out of phase with one another. If the two are the same size and a quarter cycle apart, the real (i.e., physical) part of the $\mathbf{E}$ vector will spin through 2π once per cycle, without changing its length, like a screw thread. Its endpoint will traverse a circle, so that this is known as *circular polarization*. Like screws, there is right and left circular polarization, but unlike screws, the names are backwards.

If the two components are not exactly equal in magnitude, or are not exactly $\pi/2$ radians apart, the vector will still rotate, but will change in length as it goes round, tracing an ellipse. This more general case is *elliptical polarization*. Circular and linear polarizations are special cases of elliptical polarization. Elliptical polarization can also be right or left handed.

1.2.9 Optical Loss

In a lossless medium, the $\mathbf{E}$ and $\mathbf{H}$ fields of a propagating wave are exactly in phase with each other. Any phase difference between them is due to absorption or gain in the

material. A material with dielectric constant $\epsilon' - i\epsilon''$ has a *loss tangent* $\delta = \epsilon''/\epsilon'$. In such a material, H lags E in phase by $\frac{1}{2}\arctan\delta$.

1.3 CALCULATING WAVE PROPAGATION IN REAL LIFE

A real optical system is too complicated to be readily described in terms of vector fields, so being practical folk, we look for an appropriate sleazy approximation. We know that in a homogeneous and time-invariant medium, all propagating light waves can be decomposed into their plane wave spectra; at each (temporal) frequency, there will be a unique set of vector plane waves that combine to produce the observed field distributions. The approximations we will use are four:

1. *Scalar Optics:* Replace vector field addition with scalar addition.
2. *Paraxial Propagation:* Use an approximate propagator (the Huyghens integral) to calculate wave propagation, limiting us to beams of small cone angles.
3. *Fourier Optics:* Use a simplistic model for how individual spatial Fourier components on a surface couple to the plane wave components of the incident light.
4. *Ray Optics:* Ignore diffraction by using an asymptotic theory valid as $\lambda \to 0$.

Analytical models, within their realm of applicability, are so much superior to numerical models in intuitive insight and predictive power that it is worth sacrificing significant amounts of accuracy to get one. Numerical models have their place—but the output is just a pile of special cases, so don't use them as a crutch to avoid hard thinking.

1.3.1 Scalar Optics

If we shine an ideal laser beam (one perfectly collimated and having a rectangular amplitude profile) through a perfect lens and examine the resulting fields near focus, the result is a complete mess. There are nonzero field components along the propagation axis, odd wiggly phase shifts, and so on, due entirely to the wave and vector nature of the fields themselves. The mess becomes worse very rapidly as the sine of the cone angle θ of the beam approaches unity. The effect is aggravated by the fact that no one really knows what a lens does, in sufficient detail to describe it accurately analytically—a real system is a real mess.

For most optical systems, we don't have to worry about that, because empirically it doesn't affect real measurements much. Instead, we use *scalar optics*. Scalar optics is based on the replacement of the six components of the true vector electromagnetic field by a single number, usually thought of as being the electric field component along the (fixed) polarization axis. In an isotropic medium, the vector wave equation admits plane wave solutions whose electric, magnetic, and propagation vectors are constant in space, so that the field components can be considered separately, which leads to the *scalar Helmholtz equation*,

$$(\nabla^2 + k^2)E = 0. \tag{1.17}$$

(This rationale is nothing but a fig leaf, of course.) Any solution of (1.17) can be decomposed in a Fourier function space of plane waves, which are identified with one Cartesian

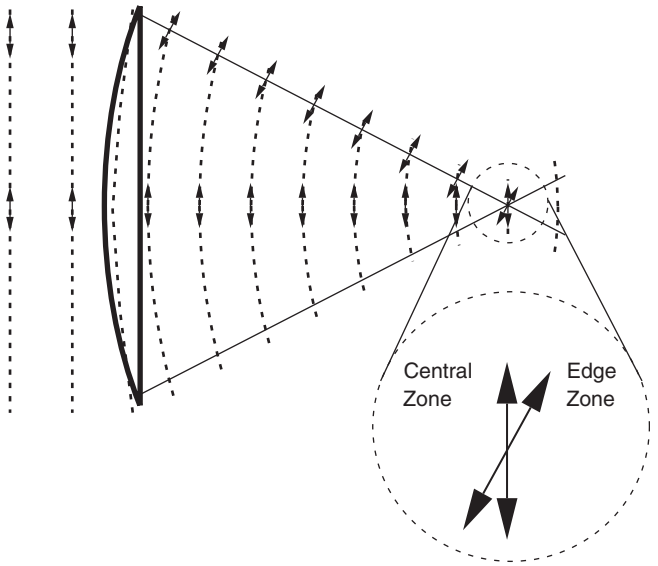

Figure 1.2. Scalar addition is a good approximation to vector addition except near high-NA foci.

component of the vector field. A scalar plane wave traveling along a direction **k** has the form

$$\psi(\mathbf{x}) = e^{i(\mathbf{k}\cdot\mathbf{x}-\omega t)}, \tag{1.18}$$

where the vector **k** has length $k = 2\pi/\lambda$. Conceptually, the true vector field can be built up from three sets of these.

The only difficulty with this in free space is that the field vectors of the plane waves are perpendicular to their propagation axes, so that for large numerical aperture,[†] where the propagation axes of the various components are very different, the vector addition of fields near a focus is not too well approximated by a scalar addition. Far from focus, this is not much of a worry, because the components separate spatially, as shown in Figure 1.2.

Aside: Plane Waves and δ-Functions. This separation is not entirely obvious from a plane wave viewpoint, but remember that plane waves are δ-functions in **k**-space; that makes them just as singular in their way as δ-functions. They aren't always an aid to intuition. Of course, it is not free space propagation that provides useful data, but the interaction of light with matter; boundaries of physical interest will in general mix the different polarization components. Such mathematical and practical objections are swept under the rug.[‡]

[†]The numerical aperture (NA) of a beam is given by $\mathrm{NA} = n\sin\theta$, where n is the refractive index of the medium and θ is the half-angle of the beam cone. By Snell's law, the numerical aperture of a beam crossing an interface between two media at normal incidence remains the same.

[‡]The actual electromagnetic boundary conditions at surfaces of interest are very complicated, and usually poorly understood, so that most of the time the inaccuracies we commit by approximating the boundary conditions are smaller than our ignorance.

Polarization and finite bandwidth effects are usually put in *by hand*. This means that we keep track of the polarization state of the beam separately and follow it through the various optical elements by bookkeeping; for frequency-dependent elements, we keep the frequency as an independent variable and integrate over it at the end. Such a procedure is inelegant and mathematically unjustified, but (as we shall see) it works well in practice, even in regimes such as high numerical aperture and highly asymmetric illumination, in which we would expect it to fail. Everyone in the optical systems design field uses it, and the newcomer would be well advised to follow this wholesome tradition unless driven from it by unusual requirements (and even then, to put up a fight).

1.3.2 Paraxial Propagation

Discussions of beam propagation, pupil functions, optical and coherent transfer functions, and point spread functions take place with reference to the plane wave basis set. There are an infinite variety of such basis sets for decomposition of solutions of the scalar Helmholtz equation, nearly none of which are actually useful. Plane waves are one exception, and the Gauss–Legendre beams are another—or would be if they quite qualified. Gaussian beams (as they are usually called) don't even satisfy the true scalar Helmholtz equation, because their phase fronts are paraboloidal rather than spherical, and because they extend to infinity in both real- and **k**- (spatial frequency) space.

Instead, they satisfy the *slowly varying envelope equation*, also known as the *paraxial wave equation*. First, we construct a field as a product of a plane wave e^{ikz} times an envelope function $\Theta(\mathbf{x})$ that varies slowly on the scale of a wavelength. This field is plugged into the scalar Helmholtz equation, the product rule for the Laplacian operator is invoked, and the subdominant term $d^2\Theta/dz^2$ is discarded, leaving a Schrödinger-type equation for the envelope Θ, the paraxial wave equation

$$\frac{d^2\Theta}{dx^2} + \frac{d^2\Theta}{dy^2} + 2ik\frac{d\Theta}{dz} = 0. \tag{1.19}$$

A general solution to this equation for all (x, y, z) is given by the *Huyghens integral*,

$$\Theta(x, y, z) = -\frac{i}{\lambda}\iint_P \Theta(x', y', z')\frac{\exp\left[ik\dfrac{(x-x')^2+(y-y')^2}{2(z-z')}\right]}{(z-z')}dx'dy', \tag{1.20}$$

where P is the $x'y'$ plane. In diffraction theory (1.20) is also known as the *Fresnel approximation*. The Huyghens integral is an example of a *propagator*, an integral operator that uses the field values on a surface to predict those in the entire space. It is slightly inconvenient to lose the explicit phase dependence on z, but that can be recovered at the end by calculating the phase of an axial ray (one traveling right down the axis of the system) and adding it in. The Huyghens kernel depends only on $\mathbf{x}-\mathbf{x}'$ and so is a convolution (see Section 1.3.8), leading naturally to a Fourier space (**k**-space) interpretation. In **k**-space, (1.20) is

$$\Theta(x, y, z) = \iint_{P'} U(u, v)e^{i(2\pi/\lambda)(ux+vy)}e^{-i(2\pi z/\lambda)[(u^2+v^2)/2]}dudv, \tag{1.21}$$

where P' is the uv plane and U is the plane wave spectrum of Θ at $z = 0$, which is given by

$$U(u, v) = \iint_P \Theta(x, y, 0) e^{-i(2\pi/\lambda)(ux+vy)} \frac{dx}{\lambda} \frac{dy}{\lambda} \tag{1.22}$$

The quantities u and v are the *direction cosines* in the x and y directions, respectively, and are related to the *spatial frequencies* k_x and k_y by the relations $u = k_x/k$, $v = k_y/k$. What we're doing here is taking the field apart into plane waves, propagating each wave through a distance z by multiplying by $\exp(ik_z z)$, and putting them back together to get the field distribution at the new plane. The (u, v) coordinates of each component describe its propagation direction. This is a perfectly general procedure.

Aside: Use k-Space. The real-space propagator (1.20) isn't too ugly, but the Rayleigh–Sommerfeld and Kirchhoff propagators we will exhibit in Section 9.3.2 are not easy to use in their real-space form. The procedure of splitting the field apart into plane waves, propagating them, and reassembling the new field is applicable to all these propagators, because in **k**-space they differ only slightly (in their *obliquity factors*, of which more later). This is really the right way to go for hand calculations.

It is actually easier to spot what we're doing with the more complicated propagators, because the $\exp(ik_z z)$ appears explicitly. The Huyghens propagator ignores the $\exp(ikz)$ factor and uses an approximation for $\exp[iz(k_z - k)]$, which obscures what's really happening.

1.3.3 Gaussian Beams

The Gauss–Legendre beams are particular solutions to the paraxial wave equation. The general form of a zero-order Gauss–Legendre beam that travels along the z axis in the positive direction and whose phase fronts are planar at $z = 0$ is

$$\Phi(x, y, z, t) = \sqrt{\frac{2}{\pi}} \frac{1}{w(z)} \exp\left\{ i\phi(z) + (x^2 + y^2)\left[\frac{-1}{w^2(z)} + \frac{ik}{2R(z)} \right] \right\}, \tag{1.23}$$

where $R(z)$, $\phi(z)$, $w(z)$, z_R, and w_0 are given in Table 1.1. (Remember that the scalar field E is the envelope Φ multiplied by the plane wave "carrier" $e^{ikz-\omega t}$.) These parameters depend only on the beam waist radius w_0 and the wavelength λ of the light in the medium.

The envelope function is complex, which means that it modulates both the amplitude and the phase ϕ of the associated plane wave. This gives rise to the curved wavefronts (surfaces of constant phase) of focused beams, and also to the less well-known variations in $\partial\phi/\partial z$ with focal position, the Gouy phase shift.

Gaussian beams reproduce the ordinary properties of laser beams of small to moderate numerical aperture. They also form a complete set of basis functions, which means that any solution of (1.19) can be described as a sum of Gaussian beams. This useful property should not be allowed to go to the user's head; Gaussian beams have a well-defined axis, and so can only represent beams with the same axis. The number of terms required for a given accuracy and the size of the coefficients both explode as the beam axis departs from that of the eigenfunctions.

TABLE 1.1. TEM_{00} Gaussian Beam Parameters (Beam Waist at $z = 0$)

Central intensity	$I_0 = 2P/(\pi w^2)$
Central intensity at the waist	$I_{0W} = 2P/(\pi w_0^2)$
Total power	$P = \pi w^2 I_0/2$
Beam waist radius (power density on axis $= I_0/e^2$)	$w_0 = \lambda/(\pi \mathrm{NA})$
$1/e^2$ Power density radius	$w(z) = w_0[1 + (z/z_R)^2]^{1/2}$
3 dB Power density radius vs. $1/e^2$ radius	$w_{1/2}(z) = 0.5887\ w(z)$
Radius within which $I >$ given I_{th}	$r = w/\sqrt{2}\ln^{1/2}(I_0/I_{\mathrm{th}})$
Power included inside $r \le w$	86.4%
99% Included power radius	$r_{99} = 1.517\ w$
Fourier transform pair	$\exp[-\pi(r/\lambda)^2] \supset \exp(-\pi \sin^2\theta)$
Separation of variables	$\exp(-\pi(r/\lambda)^2)$ $= \exp[-\pi(x/\lambda)^2]\exp[-\pi(y/\lambda)^2]$
Numerical aperture ($1/e^2$ points in **k**-space)	$\mathrm{NA} = \lambda/(\pi w_0)$
Radius of curvature of phase fronts	$R(z) = z + z_R^2/z$
Rayleigh range (axial intensity 50% of peak)	$z_R = \pi w_0^2/\lambda = \lambda/(\pi(\mathrm{NA})^2)$
Displacement of waist from geometric focus	$\Delta z \approx -z_R^2/f$
Envelope phase shift	$\phi(z) = \tan^{-1}(z/z_R)$
Equivalent projected solid angle	$\Omega'_{\mathrm{eq}} = \pi(\mathrm{NA})^2 = \lambda^2/(\pi w_0^2)$

In this book, as in most of practical electro-optical instrument design, only this lowest-order mode, called TEM_{00}, is needed. This mode describes the field distribution of a good quality laser beam, such as that from a HeNe or circularized diode laser.

At large z, the Gaussian beam looks like a spherical wave with a Gaussian cutoff in u and v, but for small z, it appears to be a collimated beam. The distance, called z_R or the Rayleigh range, over which the beam stays approximately collimated goes as $1/(\mathrm{NA})^2$—the beam waist goes as 1/NA and the the angular width as NA. At $z = \pm z_R$, the $1/e^2$ beam diameter has increased by a factor of $\sqrt{2}$, so that the central intensity has halved.

The Gaussian beam is a paraxial animal: it's hard to make good ones of high NA. Its extreme smoothness makes it exquisitely sensitive to vignetting, which of course becomes inevitable as $\sin\theta$ approaches 1, and the slowly varying envelope approximation itself breaks down as the numerical aperture increases (see Example 9.8).

There are a variety of parameters of Gaussian beams which are frequently of use, some of which are summarized in Table 1.1; P is the total power in watts, I is the intensity in $\mathrm{W/m^2}$, w is the $1/e^2$ intensity radius, w_0 is the beam waist radius, z_R is the Rayleigh range, and NA is measured at the $1/e^2$ intensity points in **k**-space. Of interest in applications is the envelope phase, which shows a $\pm\pi/4$ phase shift (beyond the plane wave's $\exp(ikz)$) over the full depth of focus (twice the Rayleigh range), so that in a focused beam it is not a good assumption that the phase is simply $\exp(ikz)$. This phase is exploited in phase contrast systems such as the Smartt interferometer.

Aside: Gaussian Beams and Lenses. When a Gaussian beam passes through a lens, it is transformed into a different Gaussian beam. For the most part, ray optics is sufficient to predict the position of the beam waist and the numerical aperture, from which the waist radius and Rayleigh range can be predicted. There are some useful invariants of

this process: for example, a Gaussian beam whose waist scans back and forth by b waist radii will be transformed into another beam whose waist scans b times the new waist radius. A position c times the Rayleigh range from the waist will image to a point c times the new Rayleigh range from the new waist. A corollary is that the number of *resolvable spots*, that is, the scan range divided by the spot diameter, is also invariant. These invariants, which are not limited to the Gaussian case, allow one to juggle spot sizes, focal positions, and scan angles freely, without having to follow them laboriously through the whole optical system.

1.3.4 The Debye Approximation, Fresnel Zones, and Fresnel Number

The plane wave decomposition of a given disturbance can be calculated from (1.22) or its higher-NA brethren in Section 9.3.6, and those work regardless of where we put the observation plane. When discussing the NA of a lens, however, we usually use a much simpler method: draw rays representing the edges of the beam and set $\mathrm{NA} = n \sin\theta$. This sensible approach, the *Debye approximation*, obviously requires the beam to be well represented by geometric optics, because otherwise we can't draw the rays—it breaks down if you put the aperture near a focus, for instance. We can crispen this up considerably via the *Fresnel construction*.

In a spherical wave, the surfaces of constant phase are equally spaced concentric hemispheres, so on a plane, the lines of constant phase are concentric circles, corresponding to annular cones, as shown in Figure 1.3. Drawing these circles at multiples of π radians divides the plane into annular regions of positive and negative field contributions, called

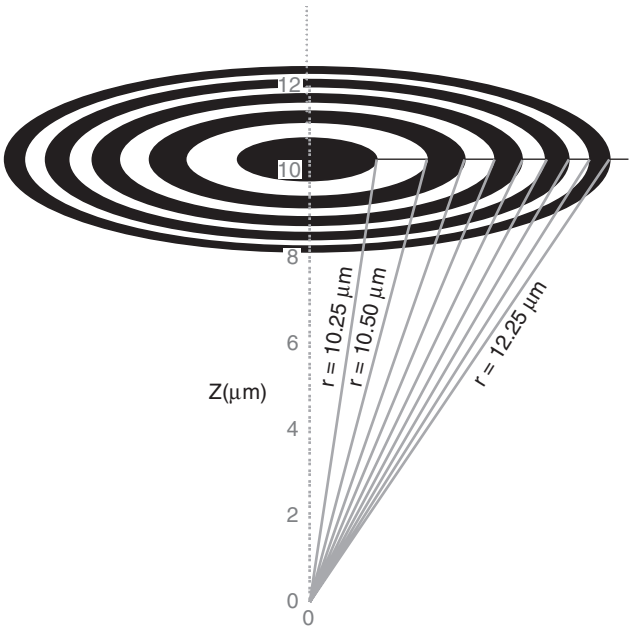

Figure 1.3. The Fresnel zone construction with $f = 10$ μm and $\lambda = 0.5$ μm. For a plane wave, taking the phase on axis as 0, alternating rings produce positive and negative field contributions at f, so blocking alternate ones (or inverting their phases with a $\lambda/2$ coating) produces a focus at f. For a converging spherical wave, all zones produce positive contributions at the focus.

Fresnel zones. The zones are not equally spaced; for a beam whose axis is along $\hat{\mathbf{z}}$ and whose focus is at $z = 0$, the angular zone boundaries in the far field are at

$$\theta_n = \cos^{-1} \frac{1}{1 + (2n+1)\lambda/(4f)} \tag{1.24}$$

(the equation for the Nth zone center is the same, except with $2N$ instead of $(2n + 1)$).

The *Fresnel number* N is the number of these zones that are illuminated. This number largely determines the character of the beam in the vicinity of the reference point—whether it is dominated by diffraction or by geometric optics. The Debye approximation is valid in the geometric limit, that is, $N \gg 1$.

Taking r to be the radius of the illuminated circle and applying a couple of trigonometric identities to (1.24) gets us a quadratic equation for N, the number of annular zone centers falling inside r. Assuming that $N\lambda \ll f$, this simplifies into

$$N = \frac{r^2}{\lambda z}, \tag{1.25}$$

which due to its simplicity is the usual definition of Fresnel number.

In small Fresnel-number situations, the focus is displaced toward the lens from its geometric position and diffraction is important everywhere, not just at the focus. The number of resolvable spots seen through an aperture of radius r is $N/2$.

Example 1.2: Gaussian Beams and Diffraction. For small numerical apertures, the position of the beam waist does not coincide with the geometric focus, but is closer. This somewhat counterintuitive fact can be illustrated by considering a beam 40λ in radius, with a lens of $10^4\lambda$ focal length placed at its waist. The lens changes the Gaussian beam parameters, as we can calculate. Geometrically, the incoming beam is collimated, so the focus is $10^4\lambda$ away, but in reality the Rayleigh range of the beam is $40(\pi/4)$ spot diameters, or 1260λ. This is only 1/8 of the geometric focal length, so the lens makes only a small perturbation on the normal diffractive behavior of the original beam. At the geometric focus, $N = 40^2/10^4 = 0.16$, so the total phase change due to the lens is only $\pi/6$ across the beam waist.

1.3.5 Ray Optics

We all know that the way you check a board for warpage is by sighting along it, because light in a homogeneous medium travels in straight lines. The departures of light from straight-line propagation arise from nonuniformities in the medium (as in mirages) and from diffraction. Most of the time these are both small effects and light can be well described by *rays*, thought of as vanishingly thin pencil beams whose position and direction are both well defined—the usual mild weirdness exhibited by asymptotic theories. Ray optics does not require the paraxial approximation, or even scalar waves.

In the absence of diffraction (i.e., as $\lambda \to 0$), the direction of propagation of a light beam in an isotropic medium is parallel to the gradient of the phase[†] $\nabla\phi$ (see

[†]M. Born and E. Wolf, *Principles of Optics*, 6th ed. (corrected). Pergamon, Oxford, 1983, p. 112.

Section 9.2.3). This means that a beam whose phase fronts are curved is either converging or diverging (see Section 9.2.2) and that rays can be identified with the normals to the phase fronts. Rays are the basis of elementary imaging calculations, as in the following example.

Example 1.3: Imaging with a Camera Lens. As a simple example of the use of ray optics, consider using a 35 mm camera to take a head-and-shoulders portrait of a friend. For portraits, the most pleasing perspective occurs with a camera-to-subject distance of a few feet, 4 feet (1.3 m) being about optimal. What focal length lens is required?

The film frame is 24 by 36 mm in size and the outline of a human head and shoulders is about 400 by 500 mm. Thus the desired magnification is 24/400, or 0.06. The rules of thin-lens optics are:

1. Rays passing through the center of the lens are undeviated.
2. Rays entering parallel to the axis pass through the focus.
3. The locus of ray bending is the plane of the center of the lens.

All of these rules can be fixed up for the thick-lens case (see Section 4.11.2). The similar triangles in Figure 1.4 show that the magnification M is

$$M = \frac{d_i}{d_o} \tag{1.26}$$

and elementary manipulation of the geometric identities shown yields

$$\frac{1}{d_o} + \frac{1}{d_i} = \frac{1}{f} \tag{1.27}$$

and

$$s_o s_i = f^2. \tag{1.28}$$

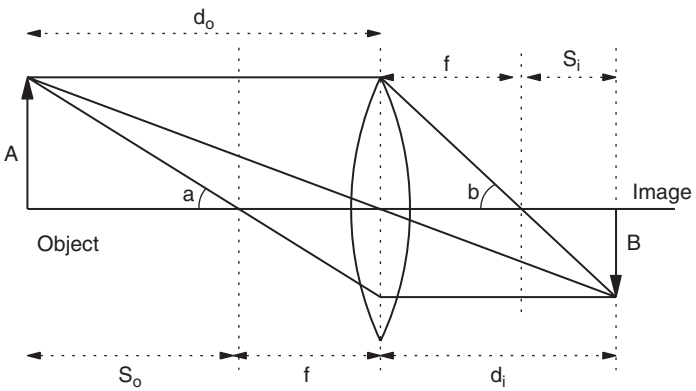

Figure 1.4. Portraiture with a 35 mm camera.

Using (1.26) and (1.27), we find that

$$f = \frac{Md_o}{1+M} \tag{1.29}$$

or 73.5 mm. Since the optimum distance is only a rough concept, we can say that a portrait lens for 35 mm photography should have a focal length of around 70 to 80 mm.

We can associate a phase with each ray, by calculating the phase shift of a plane wave traversing the same path. In doing this, we have to ignore surface curvature, in order that the wave remain plane. A shorthand for this is to add up the distances the ray traverses in each medium (e.g., air or glass) and multiply by the appropriate values of k.

1.3.6 Lenses

In the wave picture, an ideal lens of focal length f transforms a plane wave $e^{ik(ux+vy)}$ into a converging spherical wave, whose center of curvature is at (uf, vf). It does so by inserting a spatially dependent phase delay, due to propagation through different thicknesses of glass. In the paraxial picture, this corresponds to a real-space multiplication by

$$L(x, y : f) = \exp\left[\frac{i\pi}{\lambda f}(x^2 + y^2)\right]. \tag{1.30}$$

Example 1.4: A Lens as a Fourier Transformer. As an example of how to use the Huyghens propagator with lenses, consider a general field $\Theta(x, y, -f)$ a distance f behind a lens whose focal length is also f. The operators must be applied in the order the fields encounter them; here, the order is free-space propagation through f, followed by the lens's quadratic phase delay (1.30) and another free-space propagation through f. Using (1.20) twice, the field becomes

$$\Theta(x, y, +f) = \frac{i\lambda}{f}\int_{-\infty}^{\infty} d\frac{x'}{\lambda}\int_{-\infty}^{\infty} d\frac{y'}{\lambda} e^{-i(2\pi/\lambda f)(xx'+yy')}\Theta(x', y', -f), \tag{1.31}$$

which is a pure scaled Fourier transform. Thus a lens performs a Fourier transform between two planes at $z = \pm f$. If we put two such lenses a distance $2f$ apart, as shown in Figure 1.5, then the fields at the input plane are reproduced at the output plane, with a Fourier transform plane in between. The image is inverted, because we've applied two forward transforms instead of a forward $(-i)$ followed by a reverse $(+i)$ transform, so $(x, y) \to (-x, -y)$.

If we put some partially transmitting mask at the transform plane, we are blocking some Fourier components of Θ, while allowing others to pass. Mathematically, we are multiplying the Fourier transform of Θ by the amplitude transmission coefficient of the mask, which is the same as convolving it with the Fourier transform of the mask, appropriately scaled. This operation is called *spatial filtering* and is widely used.

The Fourier transforming property of lenses is extremely useful in both theory and applications. Perhaps surprisingly, it is not limited to the paraxial case, as we will see below.

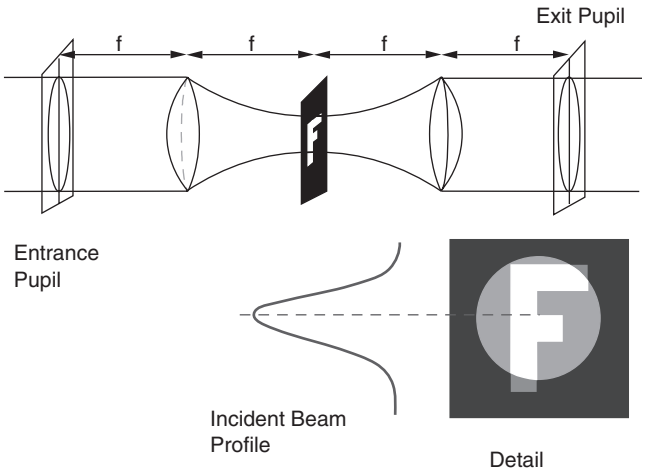

Figure 1.5. Spatial filtering.

1.3.7 Aperture, Field Angle, and Stops

Not every ray that enters an optical system will make it out the other side. At most locations in a system, there is no sharp boundary. At a given point in space, light going in some directions will make it and that going in other directions will not; similarly for a given angle, there may be part of the system where it can pass and part where it cannot. However, each ray that fails to make it will wind up hitting some opaque surface. The surface that most limits the spatial field of a ray parallel to the axis is called the *field stop* and that which limits the angular acceptance of a point on the axis most, the *aperture stop*. At these surfaces, the boundary between blocked and transmitted components is sharp. These locations are shown in Figure 1.6. It is common to put the aperture stop at a Fourier transform plane, since then all points on the object are viewed from the same range of angles. Optical systems image a volume into a volume, not just

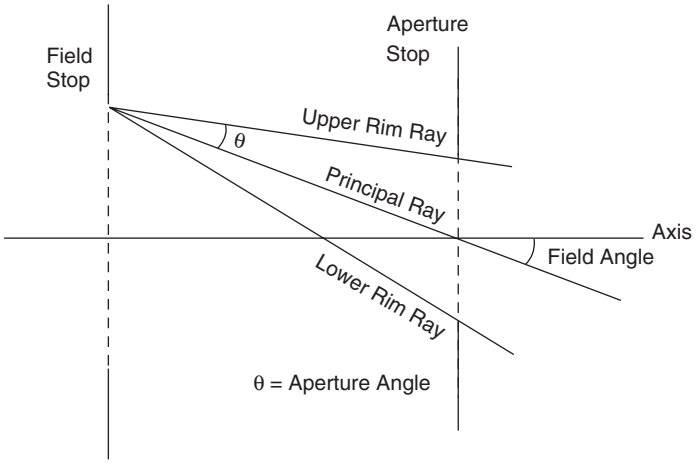

Figure 1.6. Definitions of aperture and field angle.

a plane into a plane, so the stops can't always be at the exact image and transform planes.

Aside: Vignetting. Aperture and field are defined in terms of axial points and axial rays. There's no guarantee that the aperture and field are exactly the same for other points and other directions. Rays that get occluded somewhere other than the field or aperture stops are said to have been *vignetted*. Vignetting isn't always bad—it's commonly used to get rid of badly aberrated rays, which would degrade the image if they weren't intercepted.

When a laser beam hits the edge of an aperture, it is also loosely termed vignetting, even when it does happen at one of the stops.

1.3.8 Fourier Transform Relations

Fourier transforms crop up all the time in imaging theory. They are a common source of frustration. We forget the transform of a common function or can't figure out how to scale it correctly, and what was a tool becomes a roadblock. This is a pity, because Fourier transforms are both powerful and intuitive, once you have memorized a couple of basic facts and a few theorems. In an effort to reduce this confusion, here are a few things to remember. Following Bracewell, we put the factors of 2π in the exponents and write $g \supset G$ and $G = \mathrm{F}g$ for "g has transform G:"

$$G(f) = \int_{-\infty}^{\infty} g(x) e^{-i2\pi f x} dx, \tag{1.32}$$

$$g(x) = \int_{-\infty}^{\infty} G(f) e^{i2\pi f x} df. \tag{1.33}$$

A side benefit of this is that we work exclusively in units of cycles. One pitfall is that since for a wave traveling in the positive direction, the x and t terms in the exponent have opposite signs, so it is easy to get mixed up about forward and inverse transforms. Physicists and electrical engineers typically use opposite sign conventions.

Useful Functions. The Heaviside unit step function $U(x)$ is 0 for $x < 0$ and 1 for $x > 0$. The derivative of $U(x)$ is the Dirac δ-function, $\delta(x)$. Sinc and jinc functions come up in connection with uniform beams: $\mathrm{sinc}(x) = \sin(\pi x)/(\pi x)$ and $\mathrm{jinc}(x) = J_1(2\pi x)/(\pi x)$. Even and odd impulse pairs $\mathbf{II}(x) = [\delta(x - \frac{1}{2}) + \delta(x + \frac{1}{2})]/2$ and $\mathbf{I_I}(x) = [\delta(x + \frac{1}{2}) - \delta(x - \frac{1}{2})]/2$ have transforms $\cos(\pi f)$ and $i \sin(\pi f)$, respectively.

Conjugacy. Conjugate variables are those that appear multiplied together in the kernel of the Fourier transform, such as time in seconds and frequency in hertz. In optical Fourier transforms, the conjugate variables are x/λ and u, which is as before the direction cosine of the plane wave component on the given surface, that is, $u = k_x/k$.

Convolution. A convolution is the mathematical description of what a filter does in the real time or space domain, namely, a moving average. If $g(x)$ is a given data stream and $h(x)$ is the impulse response of a filter (e.g., a Butterworth lowpass electrical filter, with x standing for time):

$$h(x) * g(x) = \int_{-\infty}^{\infty} h(\xi) g(x - \xi) d\xi = \int_{-\infty}^{\infty} g(\xi) h(x - \xi) d\xi. \tag{1.34}$$

The second integral in (1.34) is obtained by the transformation $u \to x - \xi$; it shows that convolution is commutative: $g * h = h * g$. Convolution in the time domain is multiplication in the frequency domain,

$$\mathcal{F}(h * g) = HG, \tag{1.35}$$

where capitals denote transforms, for example, $G(f) = \mathcal{F}(g(x))$. This makes things clearer: since multiplication is commutative, convolution must be too. A lot of imaging operations involve convolutions between a *point spread function* (impulse response) and the sample surface reflection coefficient (coherent case) or reflectance (incoherent case). The Huyghens propagator is also a convolution. Note that one of the functions is flipped horizontally before the two are shifted, multiplied, and integrated. This apparently trivial point in fact has deep consequences for the phase information, as we'll see in a moment. The convolution theorem is also very useful for finding the transform of a function, which looks like what you want, by cobbling together transforms that you know (see Example 1.5).

Symmetry. By a change of variable in the Fourier integral, you can show that $g(-x) \supset G(-f)$, $g^*(x) \supset G^*(-f)$, $g^*(-x) \supset G^*(f)$, and (if g is real) $G(-f) = G^*(f)$.

Correlation and Power Spectrum. The cross-correlation $g \star h$ between functions g and h is the convolution of $g(x)$ and $h^*(-x)$: $g \star h = g(x) * h^*(-x) \supset GH^*$. This can also be shown by a change of variables.

An important species of correlation is the autocorrelation, $g \star g$, whose transform is $GG^* = |G|^2$, the power spectrum. The autocorrelation always achieves its maximum value at zero (this is an elementary consequence of the Schwarz inequality) and all phase information about the Fourier components of g is lost.

Equivalent Width. We often talk about the width of a function or its transform. There are lots of different widths in common use; 3 dB width, $1/e^2$ width, the Rayleigh criterion, and so on. When we come to make precise statements about the relative widths of functions and their transforms, we talk in terms of equivalent width or sometimes autocorrelation width. The equivalent width of a function is

$$w_e(g) = \frac{\int_{-\infty}^{\infty} g(x')dx'}{g(0)} = \frac{G(0)}{g(0)}. \tag{1.36}$$

It is obvious from this that if g and G are nonzero at the origin, the equivalent width of a function is the reciprocal of that of its transform. It is this relationship that allows us to say airily that a 10-wavelength-wide aperture has an angular spectrum 0.1 rad wide.

Functions having most of their energy far from zero are not well described by an equivalent width. For example, if we move the same aperture out to $x = 200\lambda$, it will have a very large equivalent width (since $g(0)$ is very small), even though the aperture itself hasn't actually gotten any wider. Such a function is best described either by quoting its *autocorrelation width*, which is the equivalent width of the autocorrelation $g \star g$, or by shifting it to the origin. (We commonly remove the tilt from a measured wavefront, which is equivalent to a lateral shift of the focus to the origin.) Autocorrelations always achieve their maximum values at zero. Since the transform of the autocorrelation is the

power spectrum, the autocorrelation width is the reciprocal of the equivalent width of the power spectrum.

Shifting. Given $g(x)$, then shifting the function to the right by x_0 corresponds to subtracting x_0 from the argument. If $g(x)$ is represented as a sum of sinusoids, shifting it this way will phase shift a component at frequency f by fx_0 cycles:

$$\mathcal{F}(g(x - x_0)) = e^{-i2\pi f x_0} G(f). \tag{1.37}$$

Scaling. A feature 10λ wide has a transform 0.1 rad wide (in the small-angle approximation). Making it a times narrower in one dimension without changing its amplitude makes the transform a times wider in the same direction and a times smaller in height, without changing anything in the perpendicular direction:

$$g(at) \supset \frac{1}{|a|} G\left[\frac{f}{a}\right]. \tag{1.38}$$

You can check this by noting that the value of the transform at the origin is just the integral over all space of the function.

Integrating and Differentiating. For differentiable functions, if $g \supset G$, then

$$\frac{dg}{dx} \supset i2\pi f G, \tag{1.39}$$

which is easily verified by integrating by parts. If g is absolutely integrable, then

$$\int^x g \, dx' \supset \frac{G}{i2\pi f} + K\delta(f), \tag{1.40}$$

where K is an arbitrary integration constant. It follows from (1.39) that the derivative of a convolution is given by

$$\frac{d}{dx}(h * g) = h * \frac{dg}{dx} = g * \frac{dh}{dx} \supset i2\pi f G H. \tag{1.41}$$

Power Theorem. If we compute the central value of the cross-correlation of g and h, we get the odd-looking but very useful *power theorem*:

$$\int_{-\infty}^{\infty} dx \; g(x)h^*(x) = \int_{-\infty}^{\infty} df G(f) H^*(f) \tag{1.42}$$

(e.g., think of g as voltage and h as current). With the choice $g = h$, this becomes *Rayleigh's theorem*,[†]

$$\int_{-\infty}^{\infty} dx |g(x)|^2 = \int_{-\infty}^{\infty} df |G(f)|^2, \tag{1.43}$$

which says that the function and its transform have equal energy. This is physically obvious when it comes to lenses, of course.

[†]The same relationship in Fourier series is Parseval's theorem.

Asymptotic Behavior. Finite energy transforms have to fall off eventually at high frequencies, and it is useful to know how they behave as $f \to \infty$. A good rule of thumb is that if the nth derivative of the function leads to delta functions, the transform will die off as $1/f^n$. You can see this by repeatedly using the formula for the transform of a derivative until you reach delta functions, whose transforms are asymptotically constant in amplitude.

Transform Pairs. Figure 1.7 is a short gallery of Fourier transform pairs.

Example 1.5: Cobbling Together Transforms. In analyzing systems, we often need a function with certain given properties, but don't care too much about its exact identity, as long as it is easy to work with and we don't have to work too hard to find its transform. For example, we might need a function with a flat top, decreasing smoothly to zero on

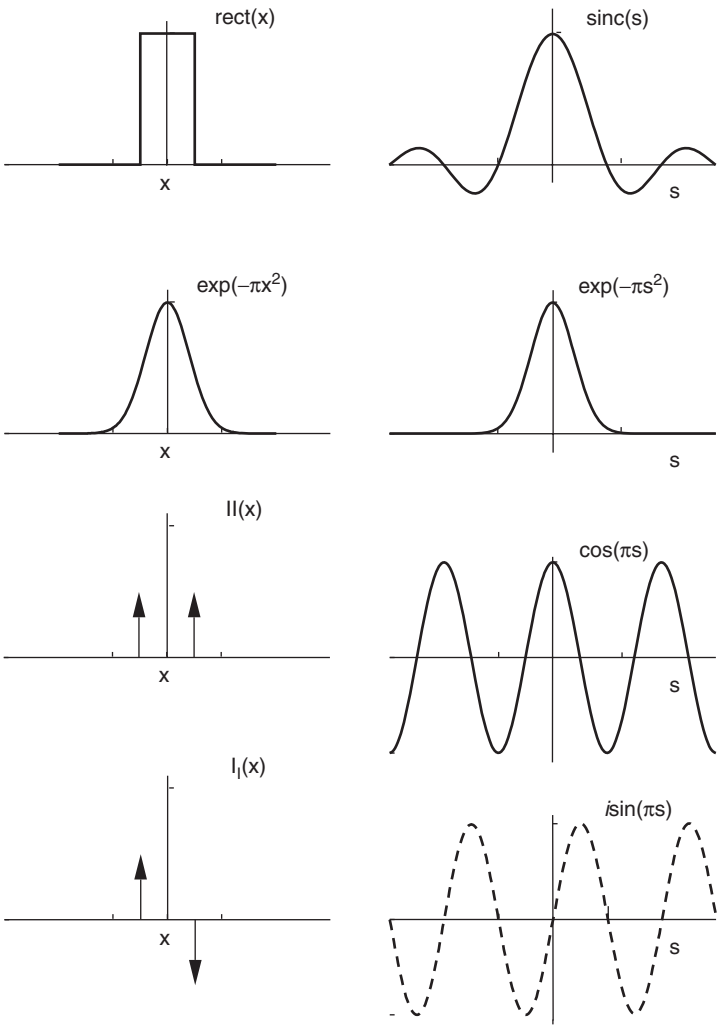

Figure 1.7. A pictorial gallery of Fourier transform pairs. Bracewell has lots more.

both sides, to represent a time gating operation of width t_g followed by a filter. The gross behavior of the operation does not depend strongly on minor departures from ideal filtering, so it is reasonable to model this function as the convolution of rect(t/t_g) with a Gaussian:

$$m(t) = \exp[-\pi(t/\tau)^2] * \text{rect}\left[\frac{t}{t_g}\right], \tag{1.44}$$

whose transform is

$$M(f) = \tau t_g e^{-\pi(f\tau)^2} \text{sinc}(f t_g). \tag{1.45}$$

One can write $m(t)$ as the difference of two error functions, but the nice algebraic properties of convolutions make the decomposed form (1.44) more useful.

1.3.9 Fourier Imaging

We have seen that a lens performs a Fourier transform between its front and back focal planes, and that in **k**-space, the propagation operator involves Fourier decomposing the beam, phase shifting the components, and reassembling them. There is thus a deep connection between the imaging action of lenses and Fourier transforms. Calculating the behavior of an imaging system is a matter of constructing an integral operator for the system by cascading a series of lenses and free-space propagators, then simplifying. Nobody actually does it that way, because it can easily run to 20th-order integrals. In a system without aberrations, we can just use ray optics to get the imaging properties, such as the focal position and numerical aperture, and then use at most three double integrals to get the actual fields, as in Example 1.4.

Most of the time, we are discussing imaging of objects that are not self-luminous, so that they must be externally illuminated. Usually, we accept the restriction to *thin objects*—ones where multiple scattering can be ignored and the surface does not go in and out of focus with lateral position. The reasoning goes as follows: we assume that our incoming light has some simple form $E_{\text{in}}(x, y)$, such as a plane wave. We imagine that this plane wave encounters a surface that has an amplitude reflection coefficient $\rho(x, y)$, which may depend on position, but not on the angle of incidence, so that the outgoing wave is

$$E_{\text{out}}(x, y) = E_{\text{in}}(x, y)\rho(x, y), \tag{1.46}$$

and then we apply the Huyghens integral to E_{out}.

Small changes in height (within the depth of focus) are modeled as changes in the phase of the reflection coefficient. Since different plane wave components have different values of k_z, we apply a weighted average of the k_z values over the pupil function. The breakdown of this procedure due to the differences in $k_z z$ becoming comparable to a cycle gives rise to the limits of the depth of focus of the beam. We ignore the possibility that the height of the surface might be multiple-valued (e.g., a cliff or overhang) and any geometric shadowing.

A very convenient feature of this model, the one that gives it its name, is the simple way we can predict the angular spectrum of the scattered light from the Fourier transform of the sample's complex reflection $\rho(x, y)$. The outgoing wave in real space is the product ρE_{in}, so in Fourier space,

$$E_{\text{out}}(u, v) = E_{\text{in}}(u, v) * P(u, v) \tag{1.47}$$

where $\rho(x/\lambda, y/\lambda) \supset P$. The real power of this is that $E_{\text{out}}(u, v)$ is also the angular spectrum of the outgoing field, so that we can predict the scattering behavior of a thin sample with any illumination we like.

If E_{in} is a plane wave, $E_{\text{in}}(x, y) = \exp[i2\pi(u_{\text{in}}x + v_{\text{in}}y)/\lambda]$, then its transform is very simple: $E_{\text{in}}(u, v) = \delta(u - u_{\text{in}})\delta(v - v_{\text{in}})$. Convolution with a shifted delta function performs a shift, so

$$E_{\text{out}}(u, v) = E_{\text{in}}(u - u_{\text{in}}, v - v_{\text{in}}). \tag{1.48}$$

The angular spectrum of E_{out} is the spatial frequency spectrum of the sample, shifted by the spatial frequency of the illumination—the spatial frequencies add. In an imaging system, the spatial frequency cutoff occurs when an incoming wave with the largest positive u is scattered into the largest negative u the imaging lens can accept.[†] Since $u^2 + v^2 \leq (\text{NA})^2$, if the NAs of the illumination and the collecting lenses are equal, the highest spatial frequency an imaging system can accept is 2 NA/λ.

The conceptual deficiencies of this procedure are considerable, even with thin objects. It works fine for large holes punched in a thin plane screen, but for more complicated objects, such as transparent screens containing phase objects (e.g., microscope slides), screens with small features, or nearly anything viewed in reflection, the approximations become somewhat scalier. The conceptual problem arises right at the beginning, when we assume that we know *a priori* the outgoing field distributions at the boundary.

There is no real material that, even when uniform, really has reflection or transmission coefficients independent of angle and polarization at optical frequencies, and the situation is only made worse by material nonuniformity and topography. This and the scalar approximation are the most problematic assumptions of Fourier optics; paraxial propagation is a convenience in calculations and not a fundamental limitation (see Section 9.3.5).

1.3.10 The Pupil

As anyone who has ever been frustrated by an out-of-focus movie knows, the image plane of an optical system is rather special and easily missed. Some other special places in an optical system are less well known. The most important of these is the *pupil*, which is an image of the aperture stop. If we look into the optical system from the object side, we see the *entrance pupil*. Looking from the image side, we see the *exit pupil*. By moving from side to side, we can locate the position in space of a pupil by how it moves in response. (This is the same way we tell how far away anything appears.)

There's nothing magical about pupils, although they are talked about in terms that may confuse newcomers—they really are just places in an optical system, which can be imaged where you want them and otherwise manipulated just as a focal plane can.

The aperture stop is usually put at the Fourier transform plane, to avoid nonuniform vignetting. The field distribution at a pupil then is the Fourier transform of that at the object or an image, appropriately scaled and with an obliquity correction. Equivalently, the field function at the transform plane is a scaled replica of the far-field diffraction

[†]There's nothing special about the choice of axes, so the limiting resolution might be different along y or at other angles.

pattern of the object, as derived using the Huyghens integral (1.20). In an imaging system, the propagator is a convolution in space, so the imaging properties are controlled by the illumination pattern and detector sensitivity function at the transform plane. Since the transform plane is usually at the pupil, these are loosely called *pupil functions*, and are two-dimensional versions of the complex frequency response of an electronic system.[†] (They are still called pupil functions even when the transform plane is not at the pupil. Laziness is the father of invention.)

Aside: Perspective. The center of the entrance pupil (or really, of the Fourier transform plane in the object space) is the center of perspective. If you're trying to make a panoramic view using an image mosaic, you'll want both foreground and background objects to have the same perspective—because otherwise, the positions of the joints between mosaic elements would have to be different depending on the distance. You can accomplish this by rotating the camera around its center of perspective.

1.3.11 Connecting Wave and Ray Optics: *ABCD* Matrices

This section could be subtitled "How to combine optical elements without drowning in multiple integrals." In an optical system consisting of lenses, mirrors, and free-space propagation, it is possible to model the paraxial imaging properties by means of very simple transformation matrices, one for each element or air space, which are multiplied together to form a combined operator that models the entire system. Here we shall discuss the 2×2 case, appropriate for axially symmetric systems or for systems of cylindrical lenses whose axes are aligned. Generalization to 4×4 matrices is straightforward but more laborious.

In the small-angle approximation (where $\sin\theta \approx \theta$), a ray at height x above the optical axis and propagating at an angle θ measured counterclockwise from the optical axis is represented by a column vector $(x, \theta)^{\mathsf{T}}$, and it transforms as

$$\begin{bmatrix} x \\ \theta \end{bmatrix} = \begin{bmatrix} a & b \\ c & d \end{bmatrix} \begin{bmatrix} x' \\ \theta' \end{bmatrix}, \tag{1.49}$$

where the matrix *abcd* is the ordered product of the *ABCD* matrices of the individual elements. Let's do an example to see how this works.

Example 1.6: Deriving the ABCD Matrix for a Thin Lens. In the ray tracing section, we saw that a thin lens brings all rays entering parallel to the axis and that a ray passing through the center of the lens is undeviated. We can use these facts to derive the *ABCD* matrix for a thin lens, as shown in Figure 1.8. The undeviated central ray, $(0, \theta)^{\mathsf{T}}$ is unchanged, so element B must be zero and element D must be 1. The ray parallel to the axis, $(1, 0)^{\mathsf{T}}$, remains at the same height immediately following the lens, so that element

[†]The analogy depends on the Debye approximation, so the exponential in/exponential out property of linear systems doesn't hold as accurately in Fourier optics as in most circuits, but it's still pretty good if the Fresnel number is high.

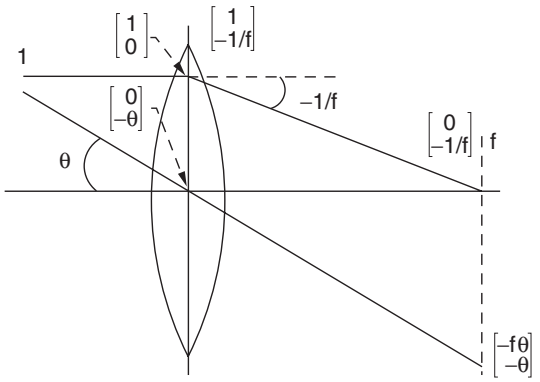

Figure 1.8. Action of a lens, for deriving its *ABCD* matrix.

TABLE 1.2. *ABCD* Matrices for Common Operations

Free-space propagation through distance z	$\begin{bmatrix} 1 & z \\ 0 & 1 \end{bmatrix}$
Thin lens of focal length f	$\begin{bmatrix} 1 & 0 \\ -1/f & 1 \end{bmatrix}$
Magnification by M	$\begin{bmatrix} M & 0 \\ 0 & 1/M \end{bmatrix}$
Fourier transform	$\begin{bmatrix} 0 & -1 \\ 1 & 0 \end{bmatrix}$

A is also 1. However, it is bent so as to cross the axis at f, so element C must be $-1/f$. Thus a thin lens has an *ABCD* matrix given in Table 1.2.

Optical layouts conventionally have light going from left to right, whereas matrix multiplication goes right to left. Thus we have to write the matrix product backwards: the *ABCD* matrix of the first element encountered by the beam goes at the right, with subsequent operations left-multiplying it in succession, as in Figure 1.9.

It is straightforward to extend this formalism to small deviations from given angles of incidence, for example, oblique reflection from a spherical mirror; when doing that, however, excellent drawings are required to avoid confusion about just what is going on.

Example 1.7: Portraiture Calculation Using ABCD Matrices. Example 1.3 demonstrated how to find elementary imaging parameters such as magnification and focal length rapidly using the thin-lens rules on rays passing through the center of the lens and rays passing through the focus. Let us follow the path of a more general paraxial ray using *ABCD* matrices. We note first that the light from the object propagates through $d_o = 1300$ mm of free space, then a thin lens of focal length $f = 73.5$ mm, and finally another free-space propagation through a distance d_i. The column vector representing the

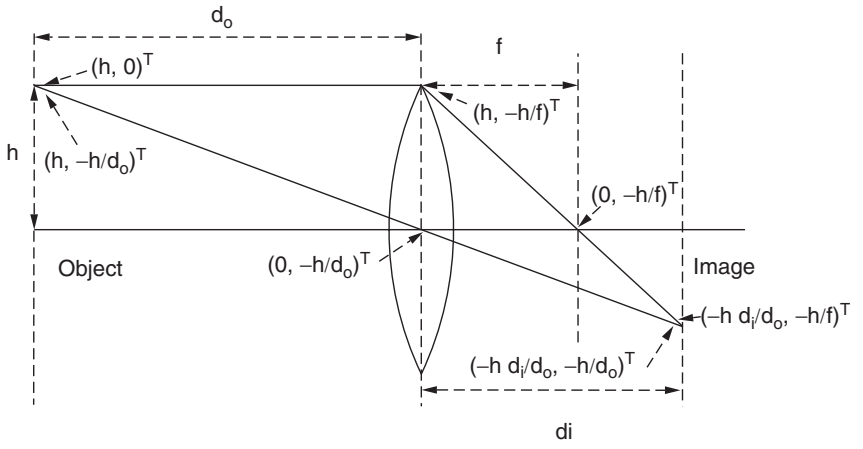

$$\begin{bmatrix} 1 & d_i \\ 0 & 1 \end{bmatrix} \begin{bmatrix} 1 & 0 \\ -1/f & 1 \end{bmatrix} \begin{bmatrix} 1 & d_o \\ 0 & 1 \end{bmatrix} = \begin{bmatrix} 1-d_i/f & d_o + d_i - d_o d_i/f \\ -1/f & 1 - d_o/f \end{bmatrix}$$

$$= \begin{bmatrix} -d_i/d_o & 0 \\ -1/f & -d_o/d_i \end{bmatrix} = \begin{bmatrix} -M & 0 \\ -1/f & -1/M \end{bmatrix}$$

Figure 1.9. Imaging geometry with ray vectors and *ABCD* matrices: rays $(h, \theta)^{\mathrm{T}}$ are successively multiplied by *ABCD* matrices corresponding to free space d_o, a lens of focal length f, and free space d_i. For the imaging condition, $1/d_o + 1/d_i = 1/f$, which makes the last three equalities true.

ray must be acted on by the matrix operators (written in reverse order as already noted):

$$\begin{aligned} \begin{bmatrix} x' \\ \theta' \end{bmatrix} &= \begin{bmatrix} 1 & d_i \\ 0 & 1 \end{bmatrix} \begin{bmatrix} 1 & 0 \\ -1/f & 1 \end{bmatrix} \begin{bmatrix} 1 & d_o \\ 0 & 1 \end{bmatrix} \begin{bmatrix} x \\ \theta \end{bmatrix} \\ &= \begin{bmatrix} 1 - d_i/f & d_o + d_i - d_i d_o/f \\ -1/f & 1 - d_o/f \end{bmatrix} \begin{bmatrix} x \\ \theta \end{bmatrix} \\ &= \begin{bmatrix} 1 - 0.0136 d_i & 1300 + 18.68 d_i \\ -0.0136 & -16.68 \end{bmatrix} \begin{bmatrix} x \\ \theta \end{bmatrix}. \end{aligned} \tag{1.50}$$

Comparing the algebraic form of the matrix product in (1.50) to the prototypes in Table 1.2, it is apparent that the combination of a lens plus free space on either side behaves as a Fourier transformer (scaled by a magnification of $-f$) when $d_o = d_i = f$. Furthermore, the imaging condition demands that all rays leaving an object point coincide at the same image point; this means that b, the (1, 2) element of the matrix, must be zero, which reproduces (1.27). These sorts of considerations are very valuable for more complex systems, where the thin-lens ray picture is cumbersome.

Useful as these are, matrix multiplication is not sufficiently powerful to model such elementary operations as the addition of a thin prism of angle ϕ and index n, which requires adding an angle $\Delta\theta = (n-1)\phi$. These matrix operators ignore wave effects and are completely unable to cope with absorbing or partially scattering objects such as beamsplitters and diffraction gratings. While these can of course be put in by hand, a more general operator algebra is desirable, which would take account of the wave nature of the light and model light beams more faithfully.

Nazarathy and Shamir[†] have produced a suitable operator algebra for Fourier optics. The key simplification in use is that they have published a multiplication table for these operators, which allows easy algebraic simplification of what are otherwise horrible high order multiple integrals. These transformations are in principle easy to automate and could be packaged as an add-on to symbolic math packages. This algebra takes advantage of the fact that commonly encountered objects such as lenses, gratings, mirrors, prisms, and transparencies can be modeled as operator multiplication in the complex field representation, which (as we have seen earlier) many cannot be so modeled in the ray representation.

Another way of coming at this is to use *ABCD* matrices for the operator algebra, and then convert the final result to a Huyghens integral. In the paraxial picture, an axisymmetric, unaberrated, unvignetted optical system consisting of lenses and free space can be expressed as a single *ABCD* matrix, and any *ABCD* matrix with $d \neq 0$ can be decomposed into a magnification followed by a lens followed by free space:

$$\begin{bmatrix} a & b \\ c & d \end{bmatrix} = \begin{bmatrix} 1 & z \\ 0 & 1 \end{bmatrix} \begin{bmatrix} 1 & 0 \\ -1/f & 1 \end{bmatrix} \begin{bmatrix} M & 0 \\ 0 & 1/M \end{bmatrix}, \tag{1.51}$$

where

$$M = \frac{1}{d}, \quad z = \frac{b}{d}, \quad f = -\frac{1}{cd}. \tag{1.52}$$

Element a does not appear because that degree of freedom is used up to ensure that the determinant of the matrix is unity, as required by the conservation of phase space volume. A magnification by M corresponds to the integral operator

$$\Theta(x, y) = \frac{1}{M} \iint dx'dy'\Theta(x', y')\delta\left[x' - \frac{x}{M}\right]\delta\left[y' - \frac{y}{M}\right]. \tag{1.53}$$

Identifying these matrix operators with the corresponding paraxial integral operators (1.20), (1.30), and (1.53), we can construct the equivalent integral operator to a general *ABCD* matrix with $d \neq 0$:

$$\Theta(x, y) = \frac{-i}{zM\lambda} \iint dx'dy'\Theta\left[\frac{x'}{M}, \frac{y'}{M}\right] \exp\left[\frac{i\pi}{\lambda}\left(\frac{(x-x')^2 + (y-y')^2}{z} + \frac{x'^2 + y'^2}{f}\right)\right]. \tag{1.54}$$

[†]M. Nazarathy and J. Shamir, First-order optics—a canonical operator representing lossless systems. *J. Opt. Soc. Am*. **72**, 356–364 (March 1982).

This transformation is simple, and it can save a *lot* of ugly integrals. The special case where $d = 0$ corresponds to a lens, followed by a scaled Fourier transform:

$$\begin{bmatrix} a & b \\ -1/b & 0 \end{bmatrix} = \begin{bmatrix} M & 0 \\ 0 & 1/M \end{bmatrix} \begin{bmatrix} 0 & -1 \\ 1 & 0 \end{bmatrix} \begin{bmatrix} 1 & 0 \\ -1/f & 1 \end{bmatrix}. \tag{1.55}$$

The constraint that $c = -1/b$ keeps the determinant 1, as before. Here the parameters are $M = -b$, $f = -b/a$ so that the equivalent integral in the wave picture is

$$\Theta(x, y) = \frac{-iM}{\lambda} \iint dx'dy'\Theta(Mx', My') \exp\left[\frac{i\pi M}{\lambda}\left(xx' + yy' + \frac{x'^2 + y'^2}{f}\right)\right]. \tag{1.56}$$

These two equivalences allow wave and ray descriptions of the same optical system to be freely interchanged, which is very convenient in calculations.

The problem of offsets, both in position and angle, can be dealt with by using the augmented vectors $[x, \theta, 1]^{\mathrm{T}}$ and 3×3 matrices. A general element producing a transformation *ABCD* and then adding an offset $[\Delta x, \Delta\theta]^{\mathrm{T}}$ is then

$$\begin{bmatrix} a & b & \Delta x \\ c & d & \Delta\theta \\ 0 & 0 & 1 \end{bmatrix}. \tag{1.57}$$

This is especially useful in getting some idea of the allowable tolerances for wedge angle, tilt, and decentration; a lens of focal length f, decentered by a distance d, adds an angular offset $\Delta\theta = d/f$. Similarly, a window of thickness t and index n, whose axis is α degrees off the normal, looks like a free-space propagation of t/n with a spatial offset of $\Delta x = \alpha t(n - 1)$. In the integral representation, offsets are modeled as convolutions with shifted δ-functions; a shift of ξ is a convolution with $\delta(x - \xi)$.

Aside: Complex ABCD Matrices and Diffraction. Siegman[†] shows that a Gaussian amplitude apodization can be modeled using the *ABCD* matrix for a thin lens with an imaginary focal length. This isn't magic, it's just that a thin lens is a multiplication by an imaginary parabolic exponential, $I(x) = \exp[i\pi x^2/(\lambda f)]$, so a Gaussian of $1/e^2$ radius w, $A(x) = \exp(-x^2/w^2)$, might be said mathematically to be a lens of focal length $i\pi w^2/\lambda$.[‡] Thus by making the first (rightmost) *ABCD* matrix a Gaussian aperture,

$$\begin{bmatrix} 1 & 0 \\ -i\lambda/(\pi w^2) & 1 \end{bmatrix}, \tag{1.58}$$

you can carry the beam radius right through the *ABCD* calculation, including converting it to a Helmholtz integral. This makes it simple to find the beam waist, for instance, and if you're building interferometers with very small diameter beams, allows you to calculate the phase front matching at the beam combiner.

[†]A. E. Siegman, *Lasers*. University Science Books, Mill Valley, CA 1986, pp. 786–797.
[‡]Note that we're using field amplitudes and not intensity here.

1.3.12 Source Angular Distribution: Isotropic and Lambertian Sources

A light source (such as the Sun) whose output is independent of direction is said to be *isotropic*; there's no special direction. Light inside an integrating sphere (Section 5.7.7) is also isotropically distributed because there's no special direction. When there's a surface involved, though, things change, on account of obliquity. If you shine a light on a perfectly matte-finished surface, its surface looks equally bright no matter what angle you look from. If you tilt it, it gets foreshortened by the perspective, but if you looked at it from a distance through a drinking straw, you wouldn't be able to tell from its brightness whether it was tilted or not. A surface that passes the drinking-straw test is said to be *Lambertian*.

If you replace your eye with a photodiode, each drinking-straw patch of surface contributes the same amount of photocurrent. As the angle increases, the patches get longer like evening shadows, so $\cos\theta$ times fewer patches will fit on the surface of the source. Another way to put this is that the total projected area of the source goes down like the cosine of the angle of incidence, so the detected photocurrent will be multiplied by the *obliquity factor* $\cos\theta$. Obliquity factors come in just about everywhere—often disguised as $\hat{\mathbf{n}} \cdot \nabla\psi$—and sometimes they seem mysterious, but all that's really going on is that shadows get longer in the evening.

1.3.13 Solid Angle

Waves expand as they propagate, but as the ray model predicts, a given wave's angular spread is asymptotically constant as $R \to \infty$. A plane angle is measured between two straight lines, so its measure doesn't depend on how far out you go. A cone has the same property in three dimensions, leading to a natural generalization, *solid angle*. The measure of a plane angle is the arc length cut out by the angle on the unit circle, so we define the solid angle of a cone to be the area it cuts out of the unit sphere. (Note that the cone need not be circular in cross section, or convex in outline, or even be a single glob—it just needs to have a shape that's independent of distance from the vertex.) This area is of course

$$\Omega = \iint_{\text{cone}} \sin\theta \, d\theta \, d\phi, \tag{1.59}$$

where θ is the polar angle (measured from the surface normal) and ϕ is the azimuth (angle in the horizon plane). In optics, we're normally calculating the flux in or out of a surface, so we have to worry about obliquity. Once again, obliquity is nothing deep or difficult to understand—when a beam of light hits a surface at an angle θ off normal, the illuminated patch is stretched out by sec θ, just as afternoon shadows of vertical objects lengthen as tan θ. Mathematically, the outward flux through each bit of surface $\mathbf{dA}$ is $\mathbf{P} \cdot \mathbf{dA}$. It simplifies matters if we fold the obliquity into the quoted solid angle, so we usually work with the *projected solid angle* Ω', where

$$\Omega' = \iint_{\text{cone}} \sin\theta \, \cos\theta \, d\theta \, d\phi. \tag{1.60}$$

To crispen this idea up, consider a circular angular pattern of half-angle ψ around the surface normal, that is, one that covers the angular disc $\theta < \psi$, $0 \le \phi < 2\pi$. Its solid angle is $\Omega = 2\pi(1 - \cos\psi) = \pi(\psi^2 - \psi^4/12 + \cdots)$ and its projected solid angle is

$\Omega' = \pi \sin^2\psi = \pi(\psi^2 - \psi^4/3 + \cdots)$. Conveniently, if $n = 1$ then $\Omega' = \pi(\mathrm{NA})^2$, which is a useful and easily remembered rule.

A Lambertian surface (one that has no preferred direction) emits into π steradians (the projected solid angle of a hemisphere). Optics folk tend to be loose about the distinction between Ω and Ω', but it isn't hard to keep straight—if the emitter or receiver is a surface, there's obliquity to worry about, so use Ω'; if not (e.g., as in gas spectroscopy) use Ω. In the usual low-NA situations, the two are equivalent for practical purposes. There are two cautions to keep in mind: first, be careful if the surface isn't flat—it's the angle between the local surface normal and the light rays that matters. Second, both solid angle and obliquity are far-field concepts, so near a focus we have to use the plane wave decomposition of the field to get the right answer.

1.3.14 Étendue: How Much Light Can I Get?

The first thing that an optical system has to be able to do is transmit light. Apart from solar telescopes, electro-optical systems are limited at least some of the time by how much light they can emit, collect, or detect. Figuring out how much you have and how much more you can get is the aim of radiometry. In Section 1.3.11, we saw that a given light beam can be focused into a smaller area, but only at the price of increasing its numerical aperture. Since $\sin\theta$ cannot exceed unity, a given beam cannot be focused arbitrarily tightly. Some beams can be focused better than others; for example, a beam from an incandescent bulb cannot be focused as tightly as one from a laser. The difference is in their degree of spatial coherence.

The spatial coherence of a beam is a measure of how well its different components (Fourier or real-space) stay in phase with each other. This is revealed by how deep the interference fringes are when different components are made to interfere with one another, as in Young's slit experiment (there's more on this in Section 2.5.4). The theory of imaging with partially coherent light is discussed by Goodman, Born and Wolf, and others and is beyond the scope of this book. As a practical matter, we usually want spatial coherence low enough to eliminate fringes in a full-field (i.e., not scanning) imaging system and high enough not to limit our ability to focus it on our area of interest. The *coherence area* of an optical field gives an idea of how far apart the slits can be and still have interference.

Conversely, one important attribute of an optical system is how well it can cope with low coherence sources. To transmit the most light from such sources, the system needs both a large area and a large angular acceptance. The figure of merit for this attribute is called the *étendue* and is given by

$$E = n^2 A\Omega', \tag{1.61}$$

where A is the clear area and n is the refractive index of the medium in which the projected solid angle Ω' is measured. It's usually just written $A\Omega'$, which assumes that $n = 1$, but we'll carry the n along explicitly. For on-axis circular pupils (the usual case), $E = n^2 A\pi(\mathrm{NA})^2$. This quantity is invariant under magnification, which increases A while decreasing Ω' proportionately, and under refraction. Étendue is a purely geometric property, which explicitly neglects the transmittance of the optical system. This is fine as long as this is reasonably uniform up to the edges of A and Ω'. It is less useful with systems whose transmittance is a strong function of angle, high-index dielectric

interfaces. The *useful* étendue is not preserved on passing through a succession of such elements, so the transmittance must be expressed as a function of position and angle, and carried along mathematically. Étendue is related to the statistical mechanics notion of phase space volume, and the conservation of étendue is the optical analogue of the conservation of phase space volume by adiabatic processes. (The *ABCD* matrices of Section 1.3.11 are all unitary, which is the paraxial version of this.)

With a given low coherence source, any two lossless optical systems with the same étendue will pass the same total optical power, if the source is matched to their characteristics with an appropriate magnification. Any mismatch will reduce the power actually transmitted. A corollary is that the étendue of a system stays the same if you send the light back through the other way. The étendue of an optical system cannot be larger than that of its poorest component, and can easily be worse due to mismatch. This is worth keeping in mind, for example, in the choice of polarizing prisms; types relying on total internal reflection (such as the Glan–Taylor) have much smaller acceptance angles than those relying on double refraction (such as Wollastons), so a bigger prism can have a smaller étendue.

Example 1.8: Étendue and Mismatch. Consider coupling sunlight into a $100\times, 0.95$ NA microscope objective ($f = 2$ mm, FOV diameter $= 100$ μm). If we shine sunlight (9 mrad angular diameter) in the pointy end, we get an effective $n^2 A\Omega'$ of $\pi(0.005 \text{ cm})^2[\pi(4.5 \text{ mrad})^2] = 5 \times 10^{-9}$ cm$^2 \cdot$ sr. If we turn it around, the étendue is unaltered, but we get the 6 mm diameter back element instead. The angular acceptance on the exit pupil is a few degrees, so we don't lose anything, and the effective $n^2 A\Omega'$ goes up by a factor of 3600 to 1.8×10^{-5} cm$^2 \cdot$ sr—and the source is still mismatched.

1.3.15 What Is "Resolution"?

The classical definitions of Rayleigh and Sparrow specify that two point-like objects of equal brightness are resolved if their images are separated by a defined multiple of the diameters of their diffraction discs. This definition is reasonably adequate for photographic detection, where the photon statistics do not significantly reduce the precision of the measurement.

With modern detectors, it is impossible to specify the resolution of an optical system when signal-to-noise considerations are absent. For example, for a two-point object, one can model the image as the sum of two Airy patterns, whose locations and intensities are parameters. By fitting the model to the observed data, the positions and intensities of the two sources can be extracted. With a high enough signal-to-noise ratio and a sufficiently accurate knowledge of the exact imaging characteristics of our systems, there is no clear limit to the two-point resolution of an optical system, as defined in this way. Optical lithography is another example where the "resolution limit" has repeatedly turned out not to be where it was expected, largely on account of the very high contrast of photoresist and, recently, phase shift masks and computational mask design.

What we really mean by *resolution* is the ability to look at an object and see what is there, in an unambiguous way that does not depend on our choice of model. This model-independent imaging property does degrade roughly in line with Rayleigh and Sparrow, but it is a much more complicated notion than simple two-point resolution. Most of the disagreement surrounding the subject of resolution is rooted here.

1.4 DETECTION

To calculate what an instrument will detect, we need to know how to model the operation of a photodetector. Fortunately, this is relatively simple to do, providing that the detector is reasonably uniform across its sensitive area. From a physical point of view, all detectors convert optical energy into electrical energy, and do it in a *square-law* fashion—the electrical power is proportional to the square of the optical power, with a short time average through the detector's impulse response. Throughout the rest of this chapter, we will normalize the scalar field function ψ so that the (paraxial) power function $\psi\psi^*$ has units of watts per square meter.

A general square-law detector with an input beam $\psi(\mathbf{x})$ and a responsivity $\mathcal{R}$ will produce an output signal S given by

$$S(t) = \mathcal{R} \iint \langle \psi(\mathbf{x}, t)^* \hat{\mathbf{n}} \cdot \nabla \psi(\mathbf{x})/k \rangle d^2x \tag{1.62}$$

which for small NA is

$$S(t) = \mathcal{R} \iint \langle |\psi(\mathbf{x}), t)|^2 \rangle d^2x, \tag{1.63}$$

where angle brackets denote time averaging through the temporal response of the detector and the integral is over the active surface of the detector. The gradient $\nabla\psi$ is parallel to the local direction of propagation (see Section 9.2.3) and the dot product supplies the *obliquity factor*, as we saw in Section 1.3.13. If the detector is seriously nonuniform, the responsivity becomes a function of $\mathbf{x}$, so $\mathcal{R}(\mathbf{x})$ must be put under the integral sign.

The square-law behavior of detectors has many powerful consequences. The first is that all phase information is lost; if we want to see phase variations, we must convert them to amplitude variations before the light is detected. Furthermore, provided that no light is lost in the intervening optical components (watching vignetting especially), the detector can in principle be placed anywhere in the receiving part of the optical system, because the time averaged power will be the same at all positions by conservation of energy. This has great practical importance, because we may need to use a small detector in one situation, to minimize dark current or ambient light sensitivity, and a large one in another, to prevent saturation and attendant nonlinearity due to high peak power levels. The small detector can be put near focus and the large one far away. This freedom applies mathematically as well; provided once again that no additional vignetting occurs, (1.63) can be applied at an image, a pupil, or anywhere convenient.[†] This becomes very useful in interferometers.

As in all interactions of light with matter, the surface properties of the detector and their variation with position, polarization, and angle of incidence are important. Fortunately, detector manufacturers endeavor to make their products as easy to use as possible, so that the worst nonuniformities are eliminated, and in addition, by the time the light gets to the detector, its numerical aperture is usually reduced sufficiently that obliquity factors and dependence on overall polarization are not too serious. As usual, they can be put in by hand if needed, so we'll continue to use the scalar model and neglect these other effects.

There are a fair number of head-scratchers associated with square-law detection. We'll talk more about it in Section 3.3.

[†]This is exact and not a Debye approximation.

1.5 COHERENT DETECTION

1.5.1 Interference

An interferometer is nothing more than a device that overlaps two beams on one detector, *coherently*, rather than combining the resulting photocurrents afterwards, *incoherently*. Coherent addition allows optical phase shifts between the beams to give rise to signal changes. In many applications the two beams are different in strength and the weaker one carries the signal information. Consequently, they are often referred to as the signal and local oscillator (LO) beams, by analogy with superheterodyne radios. Coherent detection gives the optical fields the chance to add and subtract before the square law is applied, so that the resulting photocurrent is

$$\begin{aligned} i(t) &= \mathcal{R} \iint_{\text{det}} |\psi_{\text{LO}}(\mathbf{x}) e^{-i(\omega_{\text{LO}} t + \phi_{\text{LO}}(\mathbf{x}, t))} + \psi_S(\mathbf{x}) e^{-i(\omega_S t + \phi_S(\mathbf{x}, t))}|^2 dA \\ &= i_{\text{LO}} + i_S + i_{\text{AC}}, \end{aligned} \tag{1.64}$$

assuming that the beams are polarized identically (if there are signal beam components in the orthogonal polarization state, they add in intensity, or equivalently in i). The individual
terms are

$$i_{\text{LO}} = \mathcal{R} \iint_{\text{det}} d^2x \; \psi_{\text{LO}} \psi_{\text{LO}}^*, \tag{1.65}$$

$$i_S = \mathcal{R} \iint_{\text{det}} d^2x \; \psi_S \psi_S^*, \tag{1.66}$$

and

$$\begin{aligned} i_{\text{AC}} &= 2\mathcal{R} \; \text{Re} \left\{ \iint_{\text{det}} d^2x \; \psi_{\text{LO}} \psi_S^* \right\} \\ &= 2\mathcal{R} \; \text{Re} \left\{ \exp(-i \; \Delta\omega t) \iint_{\text{det}} |\psi_{\text{LO}}(\mathbf{x})| |\psi_s(\mathbf{x})| \exp(i \; \Delta\phi(\mathbf{x}\, t)) dA \right\}. \end{aligned} \tag{1.67}$$

The first two terms, i_{LO} and i_S, are the photocurrents the two beams would generate if each were alone. The remaining portion is the *interference term*. It contains information about the relative phases of the optical beams as a function of position. The interference term can be positive or negative, and if the two beams are at different optical frequencies it will be an AC disturbance at their difference frequency $\Delta\omega$. If the two beams are superposed exactly and have the same shape (i.e., the same relative intensity distributions, focus, and aberrations), ψ_{LO} and ψ_S differ only by a common factor, so the interference term becomes

$$i_{\text{AC}} = 2\sqrt{i_{\text{LO}} i_S} \cos(\Delta\omega t + \phi). \tag{1.68}$$

Aside: Fringe Visibility. Looking at the light intensity on the detector (or on a sheet of paper), we can see a pattern of light and dark fringes if the light is sufficiently coherent.

These fringes are not necessarily nice looking. For laser beams of equal strength, they will go from twice the average intensity to zero; for less coherent sources, the fringes will be a fainter modulation on a constant background. The contrast of the fringes is expressed by their visibility V,

$$V = \frac{I_{\max} - I_{\min}}{I_{\max} + I_{\min}}, \tag{1.69}$$

which we'll come back to in Section 2.5.4 in the context of coherence theory.

1.5.2 Coherent Detection and Shot Noise: The Rule of One

Application of coherent detection to improve the signal-to-noise ratio is covered in Section 3.11.7. There are three key observations to be made here: coherent detection is extremely selective, preserves phase information, and provides noiseless signal amplification.[†] These three properties give it its power. If the two beams are exactly in phase across the entire detector, the amplitude of the interference term is twice the square root of the product of the two DC terms:

$$i_{\mathrm{AC}}(\mathrm{peak}) = 2\sqrt{i_{\mathrm{LO}} i_S}. \tag{1.70}$$

If i_S is much weaker than i_{LO}, this effectively represents a large amplification of ψ_S. The amplification is noiseless—the LO shot noise is

$$i_{N\mathrm{shot}} = \sqrt{2ei_{\mathrm{LO}}}, \tag{1.71}$$

which is exactly the rms value of i_{AC} when i_S is 1 electron per second (the noise current is down by $\sqrt{2}$ due to the ensemble average over 2π phase). Thus with $\eta = 1$, a signal beam of 1 photon/s is detectable at 1σ confidence in 1 s in a 1 Hz bandwidth, which is a remarkable result—bright-field measurements can be made to the same sensitivity as dark-field measurements.

This leads us to formulate the Shot Noise Rule of One: *One* coherently added photon per *One* second gives an AC measurement with *One* sigma confidence in a *One* hertz bandwidth. (See Sections 1.8.1 and 13.1 for more on AC versus DC measurements.)

Aside: Photons Considered Harmful. Thinking in terms of photons is useful in noise calculations but pernicious almost everywhere else—see Section 3.3.2.

1.5.3 Spatial Selectivity of Coherent Detection

If the phase relationship is not constant across the detector, fringes will form, so the product $E_{\mathrm{LO}} E_s^*$ will have positive and negative regions; this will reduce the magnitude of the interference term. As the phase errors increase, the interference term will be reduced more and more, until ultimately it averages out to nearly zero. This means that a coherent detector exhibits gain only for signal beams that are closely matched to the LO beam, giving the effect of a matched spatial filter plus a noiseless amplifier.

[†]A. V. Jelalian, *Laser Radar Systems*. Artech House, Boston, 1992, pp. 33–41.

Another way to look at this effect is to notionally put the detector at the Fourier transform plane, where the two initially uniform beams are transformed into focused spots. A phase error that grows linearly across the beam (equally spaced fringes) corresponds to an angular error, which in the transform plane means that the two focused spots are not concentric. As the phase slope increases, the spots move apart, so that their overlap is greatly reduced. Ultimately, they are entirely separate and the interference term drops to zero. Mathematically these two are equivalent, but physically they generally are not.

If the detector is placed at a focused spot, the local photocurrent density can be so large as to lead to pronounced nonlinearity; this is much less of a problem when the beams fill a substantial fraction of the detector area. On the other hand, two spots that do not overlap will not give rise to any interference term whatsoever, which is not in general true of two broad beams exhibiting lots of interference fringes; even if the broad beams are mathematically orthogonal, small variations in sensitivity across the detector will prevent their interference pattern from averaging to exactly zero.

It is hard to say exactly how serious this effect is in a given case, as it depends strongly on the details of the sensitivity variations. Sharp, strong variations (e.g., vignetting) will give rise to the largest effects, while a smooth center-to-edge variation may do nothing at all noticeable. If the application requires >40 dB (electrical) selectivity between beams at different angles, consider changing focus to separate them laterally, or relying on baffles or spatial filters as well as fringe averaging.

1.6 INTERFEROMETERS

1.6.1 Two-Beam Interferometers

Two-beam interferometers implement the scheme of Section 1.5 in the simplest way: by splitting the beam into two with a partially reflecting mirror, running the two through different paths, and recombining them. Figure 1.10 shows the heavy lifters of the interferometer world, the Michelson and Mach–Zehnder. Mach–Zehnders are more common in technological applications, because the light goes in only one direction in each arm, so it's easier to prevent back-reflections into the laser. On the other hand, a Michelson is the right choice when robust alignment is needed, because one or both mirrors can be replaced by corner cubes (don't tell anyone, but if the cubes are offset from the beam axis,

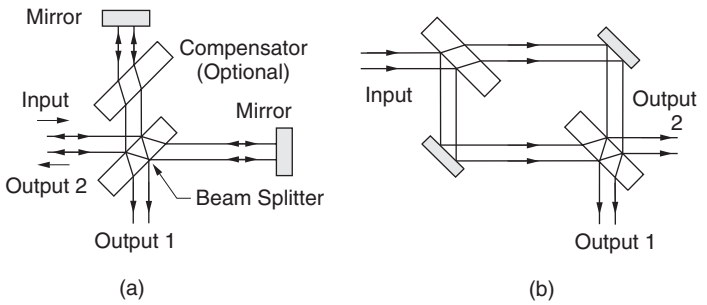

Figure 1.10. Workhorse two-beam interferometers: (a) Michelson and (b) Mach–Zehnder. The compensator plate in (a) more or less eliminates the effects of dispersion, which will smear out the white-light fringes otherwise, and also reduces the effect of finite aperture.

that's really a skinny Mach–Zehnder). Example 1.12 shows an intensive use of a corner cube type interferometer. Michelsons are a bit easier to align, because autocollimation (sending the beam back on itself) is an easy criterion to use.

An interferometer is intrinsically a four-port device; light is steered between the output ports by interference. If the two beams are perfectly coherent with one another, the output powers P_{O+} and P_{O-} from the two output ports are

$$P_{O\pm} = P_1 + P_2 \pm 2\sqrt{P_1 P_2}\cos\phi, \tag{1.72}$$

where P_1 and P_2 are the split beam powers and ϕ is the phase angle between them. The sign difference comes from beam 1 being reflected and beam 2 transmitted going into port + and vice versa for port −.

1.6.2 Multiple-Beam Interferometers: Fabry–Perots

If instead of splitting the light into multiple paths, we just take two partially reflecting mirrors and put them next to each other, parallel, we get a *Fabry–Perot* (F-P) interferometer. The multiple reflections give Fabry–Perots much greater selectivity for a given size, at the expense of far greater vulnerability to mirror errors and absorption. We'll go through the math in Section 5.4, but the upshot is that a plane-mirror F-P whose mirrors have reflectance R and are spaced d apart in a medium of index n has a total transmission

$$T_{F\text{-}P} = \frac{1}{1 + \dfrac{4R}{(1-R)^2}\sin^2(nk_0 d\cos\theta)}, \tag{1.73}$$

where θ is the angle of incidence of the beam on the mirrors (inside the medium). This obviously consists of spikes at multiples of $\Delta\nu = 1/(2nd)$, the *free spectral range* (FSR). The FWHM of the peaks is FSR/$\mathcal{F}$, where $\mathcal{F}$ is the *finesse*. Although $\mathcal{F}$ is nominally $(\pi\sqrt{R})/(1-R)$, it is really a measured quantity, because mirror flatness errors are usually the limiting factor. If the mirrors have rms error δ in waves, that limits the finesse to

$$F_{\max} < 1/(2\delta), \tag{1.74}$$

which is a pretty serious limitation most of the time—achieving a finesse of 100 requires mirror accuracy and alignment precision of better than λ/200. Real F-Ps have a peak T less than 1 (sometimes a lot less), and their total reflectance $R_{\text{F-P}}$ is less than $1 - T_{\text{F-P}}$. Recently, fabrication precision and coating quality have advanced to the point where finesse values of 2×10^5 or higher can be obtained, at a price.

Inside a F-P, the field is enhanced a great deal; the easiest way to calculate it is to notice that the forward and backward propagating fields inside the cavity are nearly equal, and that the transmitted power has to be T times the forward power. In a perfect F-P, that means that if P_{inc} is coming in, the forward power inside is $T_{\text{F-P}}/(1-R)\cdot P_{\text{inc}}$.

1.6.3 Focused-Beam Resonators

Fabry–Perots can have variable or fixed spacing; a fixed F-P is called an *etalon*. Etalons can be tuned over a small range by tipping them, but the finesse drops pretty fast when you do that since the Nth reflections start missing each other completely.

The highest finesse F-Ps are not plane-mirror devices, but rather more like laser resonators; as the finesse goes up, even small amounts of diffraction become an increasing difficulty. They need careful matching of the incoming wave to the spherical wave cavity mode, which is a big pain; fortunately, single-mode fiber coupled ones are available—buy that kind if you possibly can. Otherwise, not only do you face critical matching problems, but the minor pointing instability of the laser will turn into noise that cannot easily be removed. Fibers have their problems, but very high finesse focused F-Ps are much worse.

Aside: Confocal Cavities and Instability. It might seem that the ideal optical resonator would be a confocal cavity, where the two mirrors' centers of curvature coincide at the center of the cavity. This is not so, at least not for lasers. Such a cavity is a portion of a single sphere, and there is no special direction in a sphere—any direction is as good as any other, hence a confocal resonator has no stable axis. A tilt of ϵ radians in one mirror produces a shift of the resonator axis of $\delta\theta \approx \epsilon[L/(\Delta L)]$, where L is the distance between the mirror vertices and ΔL is the distance between their foci—which goes to ∞ as $\Delta L \to 0$. The NA of the resonant mode depends on how far off confocal the cavity is—resonant wavefronts will coincide with the cavity mirror surfaces, so NA $= 0$ for planar mirrors, NA $= 1$ for confocal mirrors, and in between, the NA can be backed out from the equation for $R(z)$ in Table 1.1. (Should ΔL be positive or negative?)

1.7 PHOTON BUDGETS AND OPERATING SPECIFICATIONS

1.7.1 Basis

Photons are like money: a certain number are needed for the job at hand, and they're easier to lose than to gain back. Thus the idea of a budget applies to photons as to finances, but it is more complicated in that not all photons are useful—as though we had to budget a mixture of green and purple dollars. A photon budget is an accounting of where photons come from, where they go, and how many are expected to be left by the time they are converted to electrons by the detector. Also like the other kind, people sometimes don't even expect to be on budget; they settle for "this was the best we could do, but I'm not sure what was the problem." In the author's experience, it is possible to achieve an SNR within 3 dB of budget almost always, and 1 dB most of the time. Don't give up, this theory stuff really works.

On the other hand, the budget must be realistic too. Don't try to measure anything in a bandwidth of less than 10 Hz, unless you have lots of cheap graduate students, and remember that you need a decent signal-to-noise ratio to actually do anything. Sensitivity limits are frequently given as *noise equivalent power* (NEP) or *noise equivalent temperature difference* (NEΔT or NETD), meaning the amount of signal you need in order to have a signal-to-noise ratio of 1, or equivalently a confidence level of 1 σ (68%). Don't let this convince you that an SNR of 1 is useful for anything, because it isn't. Generally for any reasonable measurement you need an SNR of at least 20 dB—even to do a single go/no-go test with a reasonable false call probability, you'll need at least 10 or 15 dB (3–5 σ). Tolerable images need at least 20 dB SNR; good ones, about 40 dB. Just how large an SNR your measurement has to have is a matter of deepest concern, so it should be one of the first things on the list. Don't rely on a rule of thumb you don't understand fully, including this one. There's lots more on this topic in Section 13.6.

Arriving at a photon budget and a set of operational specifications is an iterative process, as the two are inseparably linked. As the concepts are simple, the subtlety dwells in the actual execution; we will therefore work some real-life examples. The first one will be a shot-noise-limited bright-field system; the second, a background-limited dark-field system, and the third, an astronomical CCD camera. Before we start, you'll need to know how to combine noise sources (see Section 13.6.7) and to think in decibels.

Aside: Decibels. One skill every designer needs is effortless facility with decibels. There are just two things to remember: first, *decibels always measure power ratios, never voltage*. $G(\text{dB}) = 10\log_{10}(P_2/P_1)$ (we'll drop the subscript from now on and use "ln" for natural log). That formula with a 20 in it is a convenience which applies only when the impedances are identical, for example, a change in the noise level at a single test point. If you don't remember this, you'll start thinking that a step-up transformer has gain. Second, you can do quick mental conversions by remembering that a factor of two is 3 dB (since $\log_{10}(2) \approx 0.3010$), a factor of 10 is 10 dB, and $\pm$ 1 dB is 1.25× or 0.8× (since $10^{0.1} \approx 1.259$). For example, if you're looking at the output of an amplifier, and the noise level changes from 10 mV to 77 mV, that's about an 18 dB change: you get 80 from 10 by multiplying by 10 and dividing by 1.25 (20 dB − 2 dB, remembering that dB measure power), or by multiplying by 2 three times (6 + 6 + 6 = 18).

Example 1.9: Photon Budget for a Dual-Beam Absorption Measurement. One way of compensating for variations in laser output is to use two beams, sending one through the sample to a detector and the other one directly to a second detector for comparison. A tunable laser (e.g., Ti:sapphire or diode) provides the light. The desired output is the ratio of the instantaneous intensities of the two beams, uncontaminated by laser noise, drift, and artifacts due to etalon fringes or atmospheric absorption. For small absorptions, the beams can be adjusted to the same strength, and the ratio approximated by their difference divided by a calibration value of average intensity,

$$\epsilon = \frac{n_{\text{sig}}(\lambda, t)}{n_{\text{comp}}(\lambda, t)} - 1 \approx \frac{n_{\text{sig}}(\lambda, t) - n_{\text{comp}}(\lambda, t)}{\langle n_{\text{comp}}(\lambda)\rangle}, \tag{1.75}$$

where n_{sig} and n_{comp} are the photon flux (s^{-1}) in the beams. The total electrical power in the signal part is

$$P_{\text{sig}} = [\eta e(n_{\text{sig}} - n_{\text{comp}})]^2 R_L. \tag{1.76}$$

In the absence of other noise sources, shot noise will set the noise floor:

$$i_{N\text{shot}} = e\sqrt{2\eta(n_{\text{comp}} + n_{\text{sig}})}. \tag{1.77}$$

For 1 mW per beam at 800 nm and $\eta = 1$, this amounts to a dynamic range (largest electrical signal power/noise electrical power) of 150 dB in 1 Hz, or a 1σ absorption of 3 parts in 10^8. Real spectrometers based on simple subtraction are not this good, due primarily to laser noise and etalon fringes. Laser noise comes in two flavors, intensity and frequency; it's treated in Section 2.13.

Laser noise cancelers use subtraction to eliminate intensity noise and actually reach this shot noise measurement limit (see Sections 10.8.6 and 18.6.3). When frequency noise is a problem (e.g., in high resolution spectroscopy) we have to stabilize the laser.

Frequency noise also couples with the variations in the instrument's T versus λ to produce differential intensity noise, which in general cannot be canceled well. If the instrument's optical transmittance is T and the laser has a (one-sided) FM power spectrum $S(f_m)$ (which we assume is confined to frequencies small compared to the scale of T's variation), FM-AM conversion will contribute rms current noise $i_{N\text{fa}}$:

$$i_{N\text{fa}}(f) = n\eta e S(f)\frac{dT}{d\nu}. \tag{1.78}$$

If this noise source is made small, and the absorption can be externally modulated, for example, by making the sample a molecular beam and chopping it mechanically, the shot noise sensitivity limit can be reached fairly routinely. Note that this is not the same as a measurement accuracy of this order; any variations in T or drifts in calibration will result in a multiplicative error, which, while it goes to zero at zero signal, usually dominates when signals are strong.

Example 1.10: Photon Budget for a Dark-Field Light Scattering System. Many systems (e.g., laser Doppler anemometers) detect small amounts of light scattered from objects near the waist of a beam. Consider a Gaussian beam with $P = 0.5$ mW and 0.002 NA at 633 nm. From Table 1.1, the 3 dB beam radius at the waist is 70 μm, and the central intensity is $2P\pi(\text{NA})^2/\lambda^2 = 3.1 \times 10^4$ W/m^2, which is 1.0×10^{23} photons/m^2/s. A sufficiently small particle behaves as a dipole scatterer, so that the scattered light intensity is zero along the polarization axis, and goes as the sine squared of the polar angle θ. It will thus scatter light into 2π steradians, so if the total scattering cross section of the particle is σ_{tot}, the averaged scattered flux through a solid angle Ω (placed near the maximum) will be $F = 1.0 \times 10^{23}\sigma_{\text{tot}}\Omega/(2\pi)$. (Larger particles exhibit significant angular structure in their scattering behavior, with a very pronounced lobe near the forward direction.) A 1 cm diameter circular detector at a distance of 5 cm from the beam waist will subtend a projected solid angle of $\Omega' = \pi(\text{NA})^2 = \pi(0.5/5)^2 \approx 0.03$. A particle crossing the beam waist will thus result in $N = 5 \times 10^{21}\sigma_{\text{tot}}$ photons/s.

If the detector is an AR-coated photodiode ($\eta \approx 0.9$) with a load resistor $R_L = 10$ MΩ, then in a time t (bandwidth $1/(2t)$ Hz), the 1 Hz rms Johnson noise current $(4kTB/R)^{1/2}$ is $(2kT/10^7)^{1/2}$, which is 0.029 pA or 1.8×10^5 electrons/s (which isn't too good).

From Section 13.6.15, we know that in order to achieve a false count rate R of 1 in every 10^6 measurement times, we must set our threshold at approximately 5.1 times the rms amplitude of the additive Gaussian noise (assuming that no other noise source is present). Thus a particle should be detectable in a time t if σ_{tot} exceeds

$$\sigma_{\min} = \frac{1.8 \times 10^5}{5 \times 10^{21}}\frac{(5.1)}{\eta\sqrt{t}} = \frac{1.8 \times 10^{-16}}{\eta\sqrt{t}}, \tag{1.79}$$

where η is the quantum efficiency. A particle moving at 1 m/s will cross the 140 μm 3-dB diameter of this beam in 140 μs, so to be detectable it will need a scattering cross section of at least 1.6×10^{-14} m^2, corresponding to a polystyrene latex (PSL) sphere ($n = 1.51$) of about 0.2 μm diameter.

Now let's sanity-check our assumptions. For the circuit to respond this fast, the time constant $C_{\text{det}}R_L$ must be shorter than 100 μs or so, which limits the detector capacitance to 10 pF, an unattainable value for such a large detector. Even fast detectors are generally limited to capacitances of 50 pF/cm^2, so assuming the detector capacitance is actually

100 pF, we cannot measure pulses faster than 1 to 2 ms with our system as assumed. There are circuit tricks that will help considerably (by as much as 600×, see Section 18.4.4), but for now we'll work within this limit. If we can accept this speed limitation, and the accompanying ∼10× decrease in volumetric sampling rate, we can trade it in for increased sensitivity; a particle whose transit time is 2 ms can be detected at $\sigma_{\min} = 4 \times 10^{-15}$ m^2. If the particle is much slower than this, its signal will start to get down into the $1/f$ noise region, and non-Gaussian noise such as popcorn bursts will start to be important. Already it is in danger from room lights, hum, and so on.

If the detector is a photon-counting photomultiplier tube (PMT, $\eta \approx 0.2$), the noise is dominated by the counting statistics, and the technical speed limitation is removed (see Section 3.6.1). However, PMTs have a certain rate of spurious *dark counts*. Dark counts generally obey Poisson statistics, so if we assume a mean rate $N_{\text{dark}} = 200$ Hz, then in a 140 μs measurement, the probability of at least one dark count is $200 \times 140\mu\text{s} \approx 0.028$. We are clearly in a different operating regime here, where the fluctuations in the dark count are not well described by additive Gaussian noise as in the previous case. From Section 13.6.16, the probability of a Poisson process of mean rate λ per second producing exactly M counts in t seconds is

$$P(M) = \frac{(\lambda t)^M e^{-\lambda t}}{M!}. \tag{1.80}$$

If we get 200 photons per second, then the probability that a second photon will arrive within 140 μs of the first one is $(0.028)e^{-0.028} \approx 0.027$, so we expect it to happen $200 \times 0.027 \approx 5.5$ times a second. Two or more additional photons will arrive within 140 μs of the first one about 0.076 times per second, and three or more additional photons only 0.0007 times per second, so if we require at least four counts for a valid event, the false count rate will be one every 20 minutes or so, which is usually acceptable. The limiting value $\sigma_{\min}$ is then

$$\sigma_{\min} \approx \frac{4}{5 \times 10^{21} \eta t} \approx \frac{8 \times 10^{-22}}{\eta t}, \tag{1.81}$$

which is about 3×10^{-17} m^2, nearly three orders of magnitude better than the photodiode, and sufficient to detect a PSL sphere of 0.08 μm (alas for particle counters, the signal goes as a^6). We can use the same Poisson statistics to predict the probability of detection, that is, $P(\geq 4 \text{ photons})$ as a function of σ_{tot}.

Besides detector capacitance, such measurements are often limited by the shot noise of light from the background, from imperfect beam dumps, or from molecular Rayleigh scatter (as in the blue sky), so that our photon budget is not a sufficient theoretical basis for the planned measurement. More detail is available in Chapter 10. In addition, we have here assumed a very simple deterministic model for signal detection in noise; any event whose nominal detected signal is greater than our threshold is assumed to be detected. This assumption is unreliable for signals near the threshold, and is dealt with in a bit more detail in Section 13.6.15. Finally, we assumed that our noise was limited by the use of a boxcar averaging function of width t, equal to the 3 dB width of the pulse. Even with *a priori* knowledge of the arrival time of the particle, this is not the optimal case; if the particles are moving faster or slower than we anticipate, a fixed averaging window may be far from optimal. This is the topic of Section 13.8.10.

Example 1.11: Photon Budget for an Astronomical CCD Camera. An astronomical telescope gathers photons from sources whose brightness cannot be controlled. It also gathers photons from Earth, due to aurora, meteors, cosmic ray bursts, scattered moonlight, and human artifacts such as street lights. Extraneous celestial sources such as the zodiacal light and the Milky Way are also important. It represents an interesting signal detection problem: the signals that it tries to pull out of random noise are themselves random noise. The inherent noisiness of the signal is of less consequence in the optical and infrared regions than in the radio region. The brightness of sky objects is quoted in logarithmic relative *magnitudes*, with respect to standard spectral filters. A look in Allen's *Astrophysical Quantities* (affectionately known as "AQ") reveals that in the "visible" (V) filter band, centered at 540 nm in the green, a very bright star such as Arcturus or α Centauri has a magnitude $m_V = 0$, and that such an object produces a total flux at the top of the atmosphere of about 3.8 nW/m^2, of which about 80% makes it to the Earth's surface. A first magnitude star ($m_V = 1.0$) is 100 times brighter than a sixth magnitude star, which is about the limit of naked-eye detection in a dark location. A one-magnitude interval thus corresponds to a factor of $100^{0.2} \approx 2.512$ in brightness.[†]

Even in a dark location, the night sky is not perfectly dark; its surface brightness in the V band is about 400 nW/m^2/sr, which at 2.3 eV/photon is about 1×10^{10} photons/s/m^2/sr. An extended object such as a galaxy will be imaged over several resolution elements of the detector, whereas a point-like object such as a star will ideally be imaged onto a single detector element. Without adaptive optics, the turbulence of the atmosphere during the (long) measurement time limits the resolution to the size of a *seeing disc* of diameter 0.25″ (arc seconds) on the best nights, at the best locations, with 1″ being more typical, and 3″–5″ being not uncommon in backyard observatories. Thus with enough pixels, even a stellar object produces an extended image, and the SNR will be limited by the fluctuations in the sky brightness in a single pixel. Each pixel subtends the same solid angle Ω on the sky, so the mean photoelectron generation rate per pixel is

$$n_{\text{tot}} = \eta \Omega A (J_{\text{sky}} + J_{\text{star}}), \tag{1.82}$$

where A is the area of the telescope objective, η is the quantum efficiency, n is in electrons/s , and J is the photon angular flux density in photons/s/m^2/sr.

There are two classes of noise source in the measurement: counting statistics of the sky photoelectrons and of the dark current, which go as $(nt)^{1/2}$, and the (fixed) readout noise q_{RO}. The electrical SNR thus is

$$\text{SNR} = \frac{(J_{\text{star}} t \eta \Omega A)^2}{\Delta n_{\text{RO}}^2 + n_{\text{dark}} t + t \eta \Omega A (J_{\text{star}} + J_{\text{sky}})}. \tag{1.83}$$

CCD pixels have a fixed *full well* capacity B, ranging from about 5×10^4 electrons for the ones used in a camcorder to 10^6 for a scientific device. Thus the maximum exposure time for a perfect device is equal to eB/i_{sky}, which is on the order of 1 week, so that the

[†]The magnitude scale goes back to the ancient Greeks—the numerical factor is weird because the log scale was bolted on afterwards and tweaked to preserve the classical magnitudes while being reasonably memorable.

well capacity is not a limitation for dim objects. The noise-equivalent photon flux density (NEΔJ) is the number of photons per second required to achieve an SNR of 1 (0 dB) in the measurement time. Setting the SNR in (1.83) to 1 yields a quadratic equation for J_{star}, whose solution is

$$\text{NE}\Delta\text{J}_{\text{star}} \approx \frac{1}{\eta\Omega A}\sqrt{\frac{n_{\text{dark}} + \eta\Omega A J_{\text{sky}}}{t} + \frac{\Delta q_{\text{RO}}^2}{t^2}}. \tag{1.84}$$

A 100 cm telescope with a 40% central obstruction (due to the secondary mirror) has an area $A = 0.66$ m^2, and an angular resolution of about 0.14 arc seconds. A commercially available V filter has a transmittance of about 0.72 at the nominal peak.[†] Assuming that the telescope itself has an efficiency of 0.8, due primarily to absorption in uncoated aluminum primary and secondary mirrors, and is used with a cooled, back-surface illuminated CCD with $\eta = 0.85$ and $B = 1.8 \times 10^5$, the end-to-end quantum efficiency of the telescope system is $\eta \approx 0.5$. A good cooled CCD has a dark current of around 1 electron per second per pixel, and rms readout noise of about 5 electrons. With this apparatus,

$$\text{NE}\Delta\text{J} \approx \frac{3}{\Omega}\sqrt{\frac{1 + 3.3 \times 10^{11}\Omega}{t} + \frac{5^2}{t^2}}. \tag{1.85}$$

This is dominated by readout noise at short exposures. At longer times, dark current fluctuations dominate for very small values of Ω but sky background fluctuations dominate for larger Ω. The largest SNR improvement comes from increasing integration time, as shown in Figure 1.11a–d which are pictures of the galaxy M100 taken by Dennis di Cicco using an 11 inch Schmidt–Cassegrain telescope at $f/6.2$ and an SBIG ST-6 CCD camera.[‡]

With an exposure time of an hour, and a 3×3 arc second pixel size (favored by many amateurs, whose CCD budgets don't run to as many pixels as the professionals'), J_{min} is 2.2×10^9, which corresponds to a surface brightness of -28 magnitudes per square arc second, which is how this is usually quoted in astronomical circles.

If we were merely users of this instrument, that would be that. However, we are the designers, so we have complete flexibility to trade off the operating parameters. What should Ω be? For detection of faint objects, we set Ω as large as is consistent with adequate image resolution, so that the photoelectrons dominate the dark current. For stellar objects, such as star clusters, we want Ω small, since if all the light from each star is going on one pixel anyway, shrinking Ω reduces the sky light while keeping the dark current and signal current the same. For a pixel size of 0.22 arc seconds, J_{min} is 1.1×10^{11}, which means that with a 1 hour exposure on a really great seeing night, we could detect a star of magnitude 25.6 with 3σ confidence. (We've left out the noise contributed by the calibration process, which may be significant if there aren't enough calibration frames—see Section 3.9.19.)

[†]Optec Corp, *Model PFE–1 Technical Manual*.

[‡]Michael V. Newberry, The signal to noise connection. *CCD Astronomy*, Summer 1994. (Copyright © 1994 by Sky Publishing). Reprinted with permission.

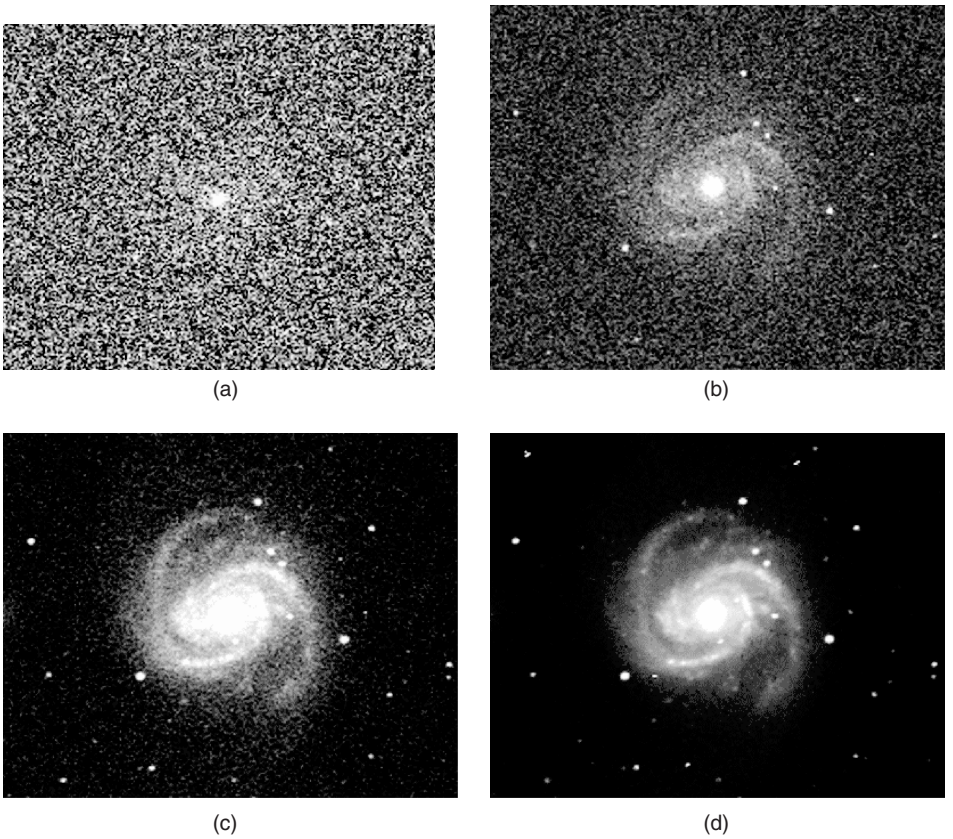

Figure 1.11. CCD image of M100: (a) 1 s integration, (b) 10 s integration, (c) 100 s integration, and (d) 1000 s integration.

1.8 SIGNAL PROCESSING STRATEGY

Once a photocurrent leaves the detector, the work of the optical system is done and the maximum SNR has been fixed by the photon budget. The signal processing job is to avoid screwing this up by needlessly rejecting or distorting the signal, on one hand, or by admitting noise unnecessarily, on the other. Signal processing operates under physical constraints, having to do with maximum allowable time delays, and practical ones such as complexity and cost. Most of the time, the inherently highly parallel data coming in as light is converted to a serial electrical channel, so that electrical wave filtering is appropriate.

1.8.1 Analog Signal Processing

The first bit of signal processing is the detector front end amplifier, in which should be included any summing or subtracting of photocurrents, for example, in a differential position measurement using a split detector. As we saw in Example 1.10, a bad front end can hobble the system by adding noise and having too narrow a bandwidth with a

given detector. Most designers are uncomfortable designing front ends, and many wind up crippling themselves by buying a packaged solution that isn't appropriate to the problem; there's detailed help available in Chapters 3 and 18.

In a baseband (near DC) measurement, the next part is usually filtering and then digitizing (AC signals will usually need frequency conversion and detection too). The filter should roll off by at least $6N$ dB (where N is the number of bits) at the Nyquist limit of the digitizer (see Section 17.4.4) and should reject strong spurious signals signals (e.g., 120 Hz from room lights) that would otherwise overwhelm subsequent stages or require more bits in the digitizer. The bandwidth of the filter should be the same as that of the signal. Although some of the signal is lost, maximum SNR occurs when the filter's frequency response is identical with the signal's power spectrum. Filters wider than that allow more noise in than necessary, and narrower ones clip off too much signal. Some filters have much better time responses than others. Have a look at the Bessel and equiripple group delay filters of Section 15.8.4. To get the best SNR with pulses, use a matched filter (Section 13.8.10).

We need to be able to convert time-domain to frequency-domain specifications. Remember that a 1 s averaging window corresponds to a bandwidth of 0.5 Hz at DC. The reason is that in the analytic signal picture negative frequencies get folded over into positive ones. However, that same 1 s window and the same folding, applied to an AC measurement, gives 0.5 Hz both above and below the (positive frequency) carrier, a total of 1 Hz. The result is that a baseband (near-DC) measurement has half the noise bandwidth[†] of an AC measurement with the same temporal response. The resulting factor of 3 dB may be confusing.

The digitizing step requires care in making sure that the dynamic range is adequate; an attractively priced 8 bit digitizer may dominate the noise budget of the whole instrument. For signals at least a few ADUs[‡] in size, an ideal digitizer contributes additive *quantization noise* of $1/\sqrt{12}$ ADU to the signal, but real A/Ds may have as much as several ADUs of technical noise and artifacts (up to $\sim$100 ADUs for $\Delta\Sigma$ ADCs, see Section 14.8.3), so check the data sheet. Converter performance will degrade by 1–3 bits' worth between DC and the Nyquist frequency. Bits lost here cannot be recovered by postprocessing, so be careful to include a realistic model of digitizer performance in your conceptual design.[§]

1.8.2 Postprocessing Strategy

With the current abundance of computing power, most measurements will include a fair bit of digital postprocessing. This may take the form of simple digital filtering to optimize the SNR and impulse response of the system, or may be much more complicated, such as digital phase-locked loops or maximum likelihood estimators of signal properties in the presence of statistically nonstationary noise and interference. In general, the difference between a simplistic postprocessing strategy and an optimal one is several decibels; this

[†]Noise bandwidth is the equivalent width of the power spectrum of the filter (see Section 13.2.5). If we put white noise into our filter, the noise bandwidth is the output power divided by the input noise power spectral density (in W/Hz), corrected for the passband insertion loss of the filter.

[‡]An ADU (analog-to-digital converter unit) is the amount of signal required to cause a change of 1 in the least significant bit of the converter.

[§]High-end oscilloscopes are a partial exception—they overcome timing skew and slew-dependent nonlinearity by calibrating the daylights out of themselves. They cost $100k and are only good to 6 bits.

may seem trivial, but remember that a 3 dB improvement in your detection strategy can sometimes save you half your laser power or 2/3 of the weight of your collection optics. (As an aside, calling it postprocessing doesn't mean that it can't be happening in real time.)

1.8.3 Putting It All Together

Let's catch our breath for a moment. We began this chapter with the aim of learning how to do a complete feasibility calculation for an optical instrument, which we should now be fully equipped to do. We have covered a lot of ground in a short time, so don't be discouraged if it takes a while for it all to slot together. It becomes easier with practice, and standing around with one or two smart colleagues doing this stuff on a white board is the most fun of any technical activity. To sum up, a conceptual design goes like this:

1. *Write down what you know*. Get a handle on the basic physics, figure out which is the largest effect operating, and estimate how much smaller the next biggest one is.
2. *Think up a measurement principle*. This may be routine, or may take a lot of imagination. Use it to take a rough cut at your photon budget. From that, estimate, for example, the laser power required, the size of the detection area needed, and so on.
3. *Simplify the analysis*. Use limiting cases, but estimate where they will break down.
4. *Make a very rough optical design*. Choose the NAs, wavelength, working distances, and so on. Check that it makes physical and economic sense.
5. *Guess a detection and signal processing strategy*. One might choose a large germanium photodiode operating at zero bias, followed by a somewhat noisy front end amplifier, a Butterworth lowpass filter, and a fixed threshold. Watch out for sources of systematic error and drift (e.g., etalon fringes or spectral changes in the source).
6. *Make a detailed photon budget*. See if your scheme will do the job, without unrealistically difficult steps.[†] If so, you have a measurement. If not, try step 5 again. If no amount of background reduction, low noise circuitry, or signal processing will help, go back to step 2 and think harder.
7. *Check it for blunders*. Do it all over again a different way, and using scaling arguments to make sure the power laws are all correct. If you go ahead with this instrument, a lot will be riding on the correctness of your calculation—don't scrimp on time and effort here. If you have one or two colleagues who are difficult to convince, try it out on them, to see if they can poke any holes in your logic.

Remember that what will get you is not misplacing a factor of Boltzmann's constant—that's large and obvious—but rather the factors of order 1 that you haven't thought out carefully. These are things like using the peak value when the rms is what's relevant, or forgetting that when you multiply two similar peaks together the result is $\sqrt{2}$ times narrower, or assuming that the bandwidth of a 1 s averaging window is 1 Hz (see

[†]As in the light bulb spectrometer of Example 17.9.

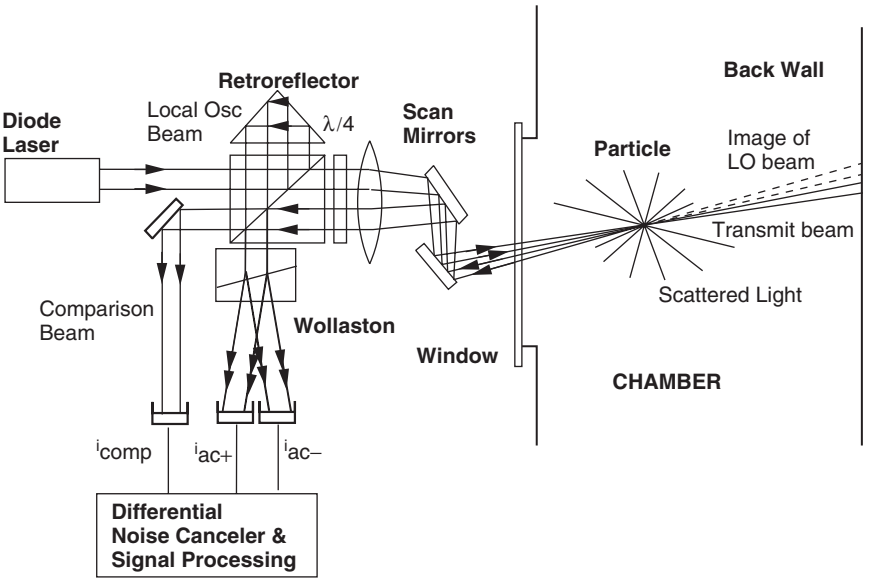

Figure 1.12. The ISICL sensor is an alignment-insensitive scanning interferometer for finding submicron particles in hostile places such as plasma chambers.

Section 13.2.5). A few of these taken together can put you off by factors of 10 or more—very embarrassing.

Estimating and controlling systematic errors is one of the high arts of the designer, since they don't obey any nice theorems as random errors sometimes do. For now we'll just try to keep the optical system simple and the processing modest and linear. Getting too far away from the measurement data is a ticket to perdition.

Let's do an extended example that illustrates many of the concepts of this chapter.

Example 1.12: Conceptual Design of a Shot-Noise-Limited, Scanning Interferometer. The ISICL (in situ coherent lidar) system[†] detects submicron ($>0.25\ \mu$m) contaminant particles in plasma chambers and other semiconductor processing equipment. As shown in Figure 1.12, it works by scanning a weakly focused laser beam around inside the chamber through a single window, and detecting the light backscattered from particles.

Backscatter operation is very difficult. Between the strong plasma glow and the stray laser light bouncing off the back wall of the chamber, it must deal with very bright stray light—thousands of times worse than that seen by an ordinary dark-field detector, and around a million times brighter than a nominally detectable particle. Coherent detection is probably the only feasible measurement strategy. With a coherent detector, a particle crossing near the focus of the beam gives rise to a short (3 μs) tone burst, whose duration is the transit time of the beam across the particle and whose carrier frequency is the Doppler shift from its radial motion. These tone bursts are filtered and amplified, then compared with a threshold to determine whether a particle event has occurred. Since

[†]P. C. D. Hobbs, ISICL: in situ coherent lidar for particle detection in semiconductor processing equipment. *Appl. Opt*. **34**(9), 1579–1590 (March 1995). Available at http://electrooptical.net/www/isicl/isiclAO.pdf.

the phase of the tone burst is random, the highest peak may be positive or negative, so bipolar thresholds are used.

The sensitivity of an instrument is expressed by the minimum number of photons it requires in order to detect a particle, which is a function of the confidence level required. A false alarm rate of 10^{-11} in the measurement time corresponds to about 1 false count per day with bipolar thresholds in a 1 MHz bandwidth. From Section 13.6.15, the false count rate depends only on the measurement bandwidth and the ratio α of the threshold to the rms noise voltage. A false count rate of 10^{-11} per inverse bandwidth requires $\alpha = 7.1$.

In an AC measurement, the shot noise level is equivalent to a single coherently detected noise photon in the measurement time, so it might seem that 7 scattered photons would be enough. Coherent detectors detect the amplitude rather than the intensity of the received light, however, so to get a signal peak 7.1 times the rms noise current, we actually need $7.1^2 \approx 50$ photons per burst.

We have a first estimate of how many photons we need, so let's look at how many we expect to get. For a particle in the center of the sensitive region, the received power is the product of the transmit beam flux density times the differential scattering cross section $\partial\sigma/\partial\Omega$ of the particle, times the detector projected solid angle Ω_d. Working in units of photons is convenient, because the relationship between photon counts and shot noise means that electrical SNR is numerically equal to the received photon count per measurement time. This works independently of the signal and filter bandwidth. Initially we ignore the losses imposed by the matched filter.

For a Gaussian transmit beam of power P at wavelength λ, focused at a numerical aperture NA, Table 1.1 gives the photon flux density at the beam waist as

$$J(P, \lambda, \mathrm{NA}) = \frac{2\pi(\mathrm{NA})^2 P\lambda}{hc}. \tag{1.86}$$

Assuming the scattered field is constant over the detector aperture, Table 1.1 predicts that the effective detector solid angle is

$$\Omega_d = \pi(\mathrm{NA})^2 \tag{1.87}$$

and so the expected number of photons available per second is

$$\langle n_0 \rangle = \frac{2\pi^2(\mathrm{NA})^4 P\lambda}{hc} \frac{\partial\sigma}{\partial\Omega}. \tag{1.88}$$

Not all of these will be detected, due to imperfect efficiency of the optics and the detector. The quantum efficiency η of the detector is the average number of detection events per incident photon on the detector; it's always between 0 and 1. (Photodetectors generally give one photoelectron per detection event, so $\eta\langle n_0 \rangle$ is the number of photoelectrons before any amplification.) A good quality, antireflection coated silicon photodiode can have $\eta \approx 0.95$ in the red and near IR, but there are in addition front surface reflections from windows and other optical losses. A receiver whose end-to-end efficiency is over 0.5 is respectable, and anything over 0.8 is very good. A value of 0.9 can be achieved in systems without too many elements, but not cheaply. (We

should also multiply by the square of the Strehl ratio to account for aberrations; see Example 9.6.)

The SNR can be traded off against measurement speed, by the choice of scanning parameters and filter bandwidths. Narrowing the bandwidth improves the time-averaged SNR but smears pulses out. In a pulsed measurement, the optimal filter is the one that maximizes the received SNR at the peak of the pulse. For pulses in additive white Gaussian noise, the optimum filter transfer function is the complex conjugate of the received pulse spectrum (this filter is not necessarily the best in real life, but it's an excellent place to start—see Section 13.8.10). Such a matched filter imposes a 3 dB signal loss on a Gaussian pulse.[†] However, the measurement detects threshold crossings, and for the weakest detectable signals, the peaks just cross the threshold. Thus this 3 dB is made up by the factor of $\sqrt{2}$ voltage gain from the peak-to-rms ratio, so that the minimum detectable number of photons (in the deterministic approximation) is still α^2.

We can estimate the stray light in the following way. Assume a detector requiring 50 photons for reliable particle identification, operating in backscatter with a 100 mW laser at 820 nm and NA = 0.008. Assume further (optimistically) that the back wall of the chamber is a perfectly diffuse (Lambertian) reflector, so that the light is scattered into π sr. The incident beam has 4×10^{17} photons/s, so that the backscattered stray light has average brightness 1.3×10^{17} photons/s/sr; the detector solid angle is $\pi(\text{NA})^2 \approx 0.0002$ sr, so the total detected signal due to stray light is about 2.6×10^{13} photons per second. Assuming that a particle takes 3 μs to yield 50 photons (1.7×10^7 photons/s), the stray light is 10^6 times more intense than the signal from a nominally detectable particle. What is worse, the signal from the back wall exhibits speckles, which move rapidly as the beam is scanned, giving rise to large (order-unity) fluctuations about the average stray light intensity. The size of the speckles (and hence the bandwidth of the speckle noise) depends on the distance from the focus to the chamber wall and on the surface finish of the wall. Peak background signals are generally much larger than this average.

The Doppler frequency shift in the detected signal due to a particle traveling with velocity $\mathbf{v}$ encountering incident light with wave vector $\mathbf{k}_i$ and scattering it into a wave with wave vector $\mathbf{k}_s$ is

$$f_d = \mathbf{v} \cdot (\mathbf{k}_s - \mathbf{k}_i)/(2\pi). \tag{1.89}$$

For a system operating in backscatter, $\mathbf{k}_s - \mathbf{k}_i \approx -2\mathbf{k}_i$. At 830 nm, a particle moving axially at 50 cm/s will give rise to a tone burst whose carrier frequency is about 1.22 MHz. This is the nominal maximum particle axial velocity for ISICL.

The remaining engineering problems center on the choice of detection bandwidths and the accurate estimation of the shot noise level in the presence of large signals due to particles. In the present case, where the Doppler shift may be large compared to the transit time bandwidth, the peak frequency of the received spectrum of a given pulse is not known in advance. The optimal signal processing system depends on the range of particle velocities expected. In quiet plasma chambers, where most particles orbit slowly within well-defined traps, the maximum expected velocity may be as low as 5 cm/s,

[†]M. Skolnik, ed., *Radar Handbook*, 2nd ed. McGraw-Hill, New York, 1990, pp. 3.21–3.23.

whereas in an environment such as a rapidly stirred fluid tank or the roughing line of a vacuum pump, the velocity range may be much greater. The scan speed of the beam focus through the inspected volume is much higher (about 20 m/s).

With carrier frequencies ranging from 0 to 1.22 MHz, the Doppler bandwidth is much larger than the transit time bandwidth (150 kHz for a 3 μs burst FWHM), so that it is inefficient to perform the thresholding operation in a single band. In the present system, four bands are used to cover the Doppler bandwidth. This is frequently best in low NA systems like ISICL, where the focus is many wavelengths across.

In a thresholding operation, it is essential to set a high enough threshold that the sensor does not report erroneously high particle counts, possibly resulting in needless down time for the processing tool being monitored. At the same time, it is economically important to use the available laser power as efficiently as possible; at the time, the laser used in this sensor cost over $1200, so that (loosely speaking) too-high thresholds cost $400 per decibel. The signal processing strategy is to set separate bipolar thresholds for each band, using an automatic thresholding circuit. This circuit exploits the accurately known noise amplitude statistics to servo on the false counts themselves and ignore signal pulses, however large they may be. In radar applications, this is known as a CFAR (constant false alarm rate) servo; the technologies employed are quite different, however, since a radar system can look at a given target many times, and its noise is very non-Gaussian. The ISICL false alarm rate (FAR) tracker can accurately servo the FAR at a level much below the true count rate in most applications.

Figure 1.13 shows a typical tone burst from a 0.8 μm diameter PSL sphere, together with cursors showing the predicted peak-to-peak voltage for a particle passing through the center of the sensing volume. For a particle exactly in focus, the photon flux predicted

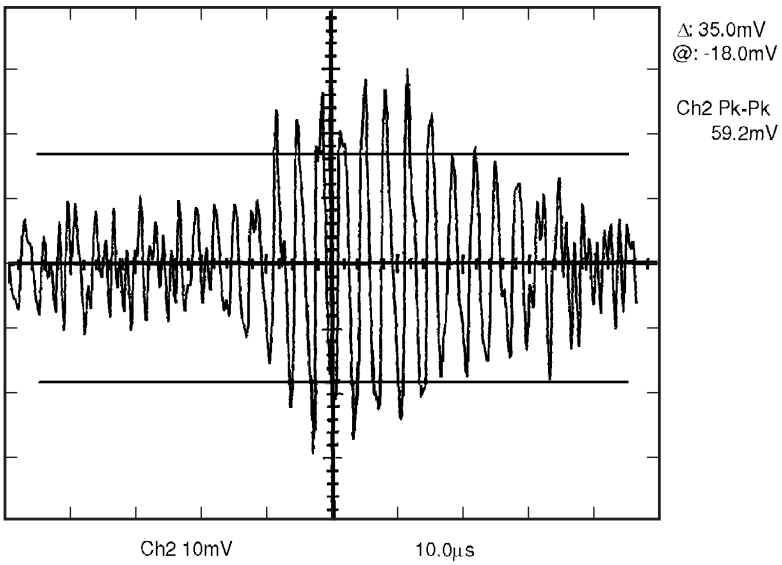

Figure 1.13. Measured tone burst caused by a 0.8 μm polystyrene latex (PSL) sphere crossing the beam near focus. The horizontal cursors are the predicted peak-to-peak value of the output. The bandwidth of the signal shown is several times wider than the actual measurement bandwidth, which prevents distortion of the tone burst but increases the noise background.

by (1.88) is converted to a signal current i_{AC} by (1.68), and to a voltage by multiplying by the known current to voltage gain (*transimpedance*) of the front end and any subsequent amplifiers. Because of the known relationship between the signal size and the shot noise in a coherent detector, we can check the ratio of the rms noise to the signal easily as well (the aberration contribution is calculated in Example 9.6). The measured system parameters are NA = 0.0045, $P = 90$ mW, $\lambda = 820$ nm, $\eta = 0.64$. Taking into account the addition of the noise and signal, the error is less than 20% (1.6 dB electrical), indicating that the theory correctly predicts the signal size and SNR.